[American Journal of Science, Vol. 311, March, 2011, P. 237–260, DOI 10.2475/03.2011.03]

SIMS ZIRCON U-Pb GEOCHRONOLOGY AND Sr-Nd ISOTOPES OF Ni-Cu-BEARING MAFIC-ULTRAMAFIC INTRUSIONS IN EASTERN TIANSHAN AND BEISHAN IN CORRELATION WITH FLOOD BASALTS IN TARIM BASIN (NW CHINA): CONSTRAINTS ON A *CA.* 280 MA MANTLE PLUME

KE-ZHANG QIN*,†, BEN-XUN SU*,†, PATRICK ASAMOAH SAKYI**, DONG-MEI TANG*, XIAN-HUA LI***, HE SUN*, QING-HUA XIAO*, and PING-PING LIU§

ABSTRACT. Zircon SIMS U-Pb dating of the Poshi, Hongshishan, Bijiashan, and Huangshan Ni-Cu-bearing and Xiangshan Ni-Cu-Ti-Fe-bearing mafic-ultramafic intrusions in the Eastern Tianshan and Beishan Rift yields a relatively restricted range of 278.6 Ma to 284.0 Ma. The histogram of compiled age data of basalts in the Tarim Basin and mafic-ultramafic intrusions in the Eastern Tianshan and Beishan Rift has a peak of 280 Ma, which probably represents the time of mantle plume activity. The basalts have lower $\varepsilon_{Nd}(t)$ values in the range of $-9.2 \sim -1.7$ and Mg# of <50, and higher TiO_2 contents (>2 wt.%), indicating that they were generated directly from a peripheral zone of the mantle plume by low degree of melting. The mafic-ultramafic intrusions have higher $\varepsilon_{Nd}(t)$ of $-1.3 \sim 11.2$ and Mg# of $33 \sim 90$, and lower $TiO_2 < 1.8$ weight percent, suggesting that their parental magmas were produced from lithospheric mantle source by high degree of melting due to higher temperature of the mantle plume head. A possible mantle plume model beneath lithospheric mantle of the Tarim Basin, Tianshan and Beishan and its spatial framework is suggested.

Key words: Beishan Rift, Eastern Tianshan, large igneous province, Ni-Cu-bearing mafic-ultramafic intrusion, mantle plume, Tarim Basin

INTRODUCTION

Large igneous provinces (LIPs) consisting of voluminous volcanic sequences (several million km^3) erupted over a relatively short time period, and are interpreted to be linked genetically with mantle plume activities (Campbell and Griffiths, 1990; Coffin and Eldholm, 1994; Chung and Jahn, 1995; Dalziel and others, 2000; Condie, 2001; Ernst and Buchan, 2003; Jourdan and others, 2009). Most plumes (and LIPs) are associated with tectonic rifts such as the Afar plume and the East Africa rift (Rogers and others, 2000), Emeishan plume and Panxi rift (Xu and others, 2001; He and others, 2003; Xiao and others, 2003, 2004a), as well as dikes, sills and layered intrusions (Ernst and Buchan, 2003) such as the abundant mafic-ultramafic intrusions distributed in the Emeishan LIP (Zhong and others, 2003; Zhong and Zhu, 2006; Zhou and others, 2008). It is well documented that the flood basalts and intrusions generated from an individual plume exhibit identical or correlated geochronological and geochemical signatures (for example, Condie, 2001; Isley and Abbott, 2002; Ernst and Buchan, 2003).

Abundant basaltic lavas widely distributed in the Tarim Basin, NW China, have been identified as a large igneous province possibly related to a mantle plume (Zhang and others, 2003; Xia and others, 2006; Yang and others, 2007a; Li and others, 2008;

* Key Laboratory of Mineral Resources, Institute of Geology and Geophysics, Chinese Academy of Sciences, P.O. Box 9825, Beijing 100029, China
** Department of Earth Science, University of Ghana, P.O. Box LG 58, Legon-Accra, Ghana
*** State Key Laboratory of Lithospheric Evolution, Institute of Geology and Geophysics, Chinese Academy of Sciences, P.O. Box 9825, Beijing 100029, China
§ Department of Earth Sciences, the University of Hong Kong, Pokfulam Road, Hong Kong, China
† Corresponding author: E-mail: kzq@mail.iggcas.ac.cn; subenxun@mail.igcas.ac.cn; Phone: +86-10-82998183; Fax: +86-10-62010846; Address: P.O. Box 9825, Beijing 100029, China

Chen and others, 2009; Zhou and others, 2009; Tian and others, 2010). However, this inference has not yet been well established because the few geochronological studies conducted on basalts yield a broad time span of 272~292 Ma (Zhang and others, 2003, 2010; Li and others, 2007; Chen and others, 2009). Furthermore, the number of geochemical investigations is limited. Intrusions are poorly exposed within the Tarim LIP, particularly in the southern part of the Tarim Basin. Since a mantle plume may have diameters of 1500~3000 km (Condie, 2001; Ernst and Buchan, 2003), distances of *ca.* 800 km to the east of the Tarim LIP might possibly lie above the possible plume. This includes field locations in Eastern Tianshan and Beishan where a number of mafic-ultramafic intrusions and associated Ni-Cu sulfide deposits occur. The Beishan Rift, located close to the northwestern Tarim Basin, is interpreted to be a rift developed in the Paleozoic (Jiang and others, 2006; Mao and others, 2008; Xu and others, 2009; Su and others, 2010a, 2010b, 2010c, 2010d) and probably associated with the mantle plume activity (Zhou and others, 2004; Su and others, 2010b).

Late Paleozoic is a key tectonic evolutional stage for Central Asian Orogenic Belt. At that period, Paleo-Asian Ocean was almost closed, and subsequently orogenesis and magmatism became more active accompanied by large-scaled metallogenesis (for example, Qin and others, 2002a, 2002b, 2003, 2005; Xia and others, 2004, 2006; Xiao and others, 2009; Zhang and others, 2010). It is little known about the proportion of contributions from the Early Permian mantle plume to the above events. In this aspect, it will be an important work to probe and constrain the plume activity in the southern Central Asian Orogenic Belt. In this paper, we investigate some of the Ni-Cu-bearing mafic-ultramafic intrusions in the Eastern Tianshan and Beishan Rift, and present zircon SIMS U-Pb age and Sr-Nd isotopic data as well as compiled results from previous studies, to understand the correlation between the Tarim flood basalts and mafic-ultramafic intrusions, and to provide geochronological and isotopic constraints on the mantle plume.

Geological background and Ni-Cu-bearing mafic-ultramafic intrusions

The Tarim Basin, located in NW China, is bounded by the Tianshan Mountains to the north and west, and the West Kunlun and Altun Mountains to the south (fig. 1). A Precambrian basement composed of Archean and Proterozoic crystalline rocks is overlain by a thick sedimentary sequence (BGMRXUAR, 1993). Drilling activities in the Tarim Basin have revealed that the basin is underlain by Permian basalts at a depth of about 200 m. The basalts occupy a minimum area of 200,000 km^2 and have tens to hundreds of meters of thickness (fig. 1; Yang and others, 2005; Chen and others, 2006). It is worthy to note that the defined basalt field in figure 1 represents the minimum distribution in the basin. Some mafic dikes, mainly syenites, occur on the margins of the basin, such as Bachu and Yingmai intrusions (fig. 1; Chen and others, 1999; Zhang and others, 2008, 2010; Zhou and others, 2009). The detail descriptions of the Tarim Basin are available elsewhere (for example, Chen and others, 2006; Yang and others, 2007b; Li and others, 2008; Zhang and others, 2008; Zhou and others, 2009; Tian and others, 2010).

The Eastern Tianshan, the eastern part of the Tianshan Mountains, forms a part of the Central Asian Orogenic Belt (Xia and others, 2006). It is one of the most important Ni-Cu metallogenic provinces in China (Qin and others, 2003, 2009). There are two main tectonic units of the Eastern Tianshan: the Jueluotage Belt and the Middle Tianshan Massif, separated by the Aqikekuduke-Shaquanzi fault (fig. 2). The Jueluotage Belt is composed of Devonian-Carboniferous volcanic rocks and tuff, sandstones and pelitic slates with interlayered limestones, mudstones, siltstones and conglomerates all of which have been subjected to late-stage low grade metamorphism and exhibit cleavage. The Middle Tianshan Massif, on the other hand, is composed of Precambrian crystalline basement (BGMRXUAR, 1993; Qin and others, 2002a; Tang

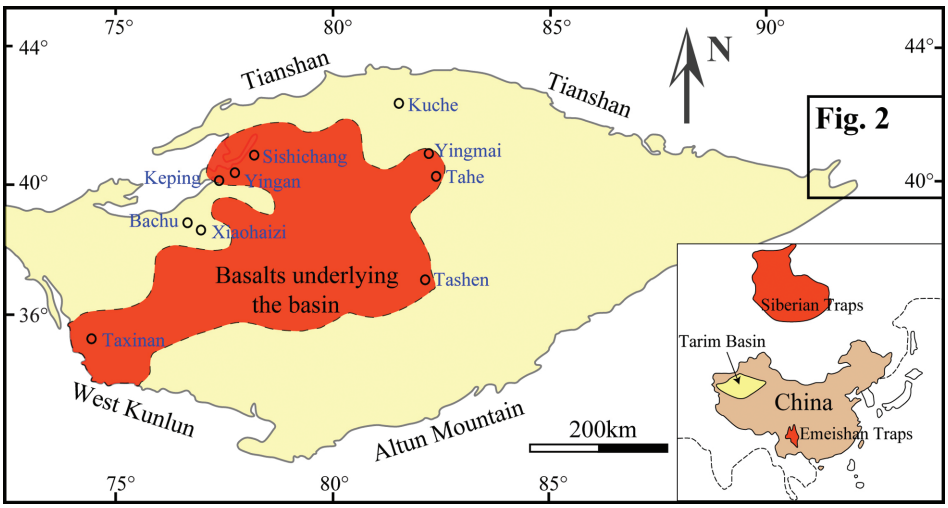

Fig. 1. Geological map of the Tarim Basin (NW China) showing the minimum distribution of Early Permian basalts (modified after Yang and others, 2005; Zhou and others, 2009). Note that the defined basalt field represents the minimum distribution in the basin.

others, 2009; Su and others, 2010b, 2010e). Permian mafic-ultramafic intrusions are distributed along the northern margin of the Middle Tianshan Massif and within the Kanggur-Huangshan ductile shear zone, a sub-unit of the Jueluotage Belt (fig. 2). The irregular-shaped sills or dikes of the mafic-ultramafic intrusions generally extend west

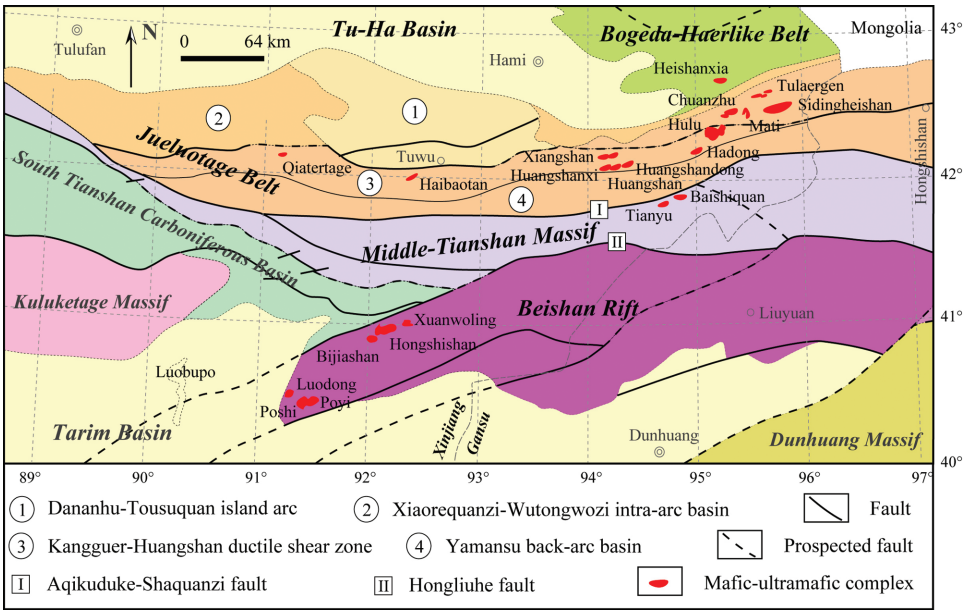

Fig. 2. Geological map of the Eastern Tianshan and Beishan rift showing the distribution of Early Permian mafic-ultramafic complexes (modified after Su and others, 2010b). Note that many non-studied intrusions are not illustrated here.

to east with an area of less than 3 km^2 (table 1; Qin and others, 2002a, 2009; Zhou and others, 2004; Jiang and others, 2006; Pirajno and others, 2008; Mao and others, 2008; Su and others, 2009, 2010c, 2010d). Generally, ultramafic rocks are set in the center of the complexes and are surrounded by mafic bodies. The constituent rocks range from diorite and hornblende/olivine gabbro, to ultramafic rocks such as (olivine) pyroxenite, pyroxene peridotite and dunite (table 1). The intrusive rocks in the Eastern Tianshan are variably altered, usually containing hydrous minerals such as hornblende and biotite, and host Ni-Cu sulfide deposits (Qin and others, 2003, 2007, 2009; Zhou and others, 2004; Sun and others, 2007; Chai and others, 2008; Tang and others, 2009; Han and others, 2010). Parts of many of the mafic-ultramafic intrusive complexes host Ni-Cu sulfide deposits. The Huangshan, Haungshandong and newly discovered Tulaergen deposits are the three largest Ni-Cu deposits and are being mined. Massive ores are hosted by ultramafic rocks, while net-textured and disseminated ores are commonly observed in hornblende gabbro and norite (Han and others, 2010; Liu and others, 2010; Xiao and others, 2010; San and others, 2010). Comprehensive studies have been done by geologists and other researchers (Qin and others, 2002a, 2003, 2007; Zhou and others, 2004; Mao and others, 2006a; Sun and others, 2006, 2007, 2009; Chai and others, 2008; Mao and others, 2008; Pirajno and others, 2008; Tang and others, 2009; Wang and others, 2009; Xiao and others, 2010).

The Beishan Rift, a junction between the Tarim Basin and the Eastern Tianshan, is located to the northeast of the Tarim Basin and is bounded by the Dunhuang Terrane and the Middle Tianshan Massif, both of which have Precambrian basement (fig. 2; BGMRXUAR, 1993). Fault-related uplifts and sags are well developed and separate strata from Cambrian to Permian in the Beishan Rift (fig. 2). The Permian mafic-ultramafic intrusions so far discovered are mainly distributed in the western part of the rift and are intruded into the Carboniferous strata. In recent years, the active exploration works revealed that the Ni-Cu mineralization potential is promising. However, fundamental studies on these intrusions are very limited (Jiang and others, 2006; Su and others, 2009, 2010b, 2010c; Ao and others, 2010). These intrusions in the Beishan Rift have outcropping area of less than 15 km^2, and are markedly fresh, characterized by the presence of troctolite and low/no modal abundance of hydrous minerals, and are the sib of active exploration for Cu-Ni sulfide deposits (Jiang and others, 2006; Su and others, 2009; Ao and others, 2010). They have rock assemblages of dunite, pyroxene peridotite, troctolite, olivine gabbro and gabbro, most of which are fresh or weakly altered (Jiang and others, 2006; Su and others, 2009, 2010b, 2010d). Coeval volcanic rocks and acidic intrusions commonly coexist with the mafic-ultramafic complexes (Su and others, 2009, 2010a). Previous studies suggested that these mafic-ultramafic intrusions intruded in the Early Permian (270~290 Ma), and evolved from high-Mg basaltic magmas originating from a depleted mantle that had been metasomatized to variable extents by a subducted slab (for example, Zhou and others, 2004; Chai and others, 2008; Mao and others, 2008; Tang and others, 2009; Su and others, 2010b).

We sampled diorites (HSS12) and rhyolites (HSS6) from the Hongshishan and its adjacent region, respectively, olivine gabbros (PSZK1-2-650) from the Poshi drill hole, and gabbros (BJS-6, XSTiFe-V and HS-V) from the Bijiashan, Xiangshan and Huangshan intrusions for zircon U-Pb dating. The detailed petrological descriptions of the studied intrusions are provided elsewhere (Zhou and others, 2004; Jiang and others, 2006; Mao and others, 2008; Pirajno and others, 2008; Su and others, 2009, 2010c; Xiao and others, 2010; Han and others, 2010).

ANALYTICAL METHODS

Zircon grains were separated from the collected samples using conventional heavy liquid and magnetic techniques, and together with zircon standard TEMORA were

Table 1

Features of mafic-ultramafic complexes and associated Ni-Cu mineralization in Beishan, Mid-Tianshan and Kangurtag-Jingerquan belts

mafic-ultramafic complex	length×width (km)	scope (km^2)	ore scale	mafic-ultramafic association
Beishan				
Xuanwoling	4×2	5	in exploration	peridotite, troctolite, gabbro, olivine gabbro
Hongshishan	5.8×1.6	4.7	in exploration	peridotite, troctolite, gabbro, olivine gabbro
Bijiashan	6.8×2.6	13	in exploration	peridotite, troctolite, gabbro, olivine gabbro
Poshi	2×1.6	2.5	medium-sized Ni-Cu	plagioclase/amphibole peridotite, olivine pyroxenite, olivine/hornblende gabbro, gabbro
Luodong	2×1.2	2.0	in exploration	plagioclase/amphibole peridotite, pyroxenite, olivine gabbro, gabbro
Mid-Tianshan				
Xiadong	7×0.5	2.5	in exploration	dunite, amphibole pyroxenite, (olivine) gabbro, amphibolite
Tianyu	1.2×0.05	0.056	medium-sized Ni-Cu	peridotite, olivine/amphibole pyroxenite, gabbro
Baishiquan	2.6×0.5	0.8	medium-sized Ni-Cu	peridotite, olivine pyroxenite, troctolite, hornblende gabbro, gabbro
Kangurtag-Jingerquan				
Tulaergen	0.74×0.06	0.03	large Ni-Cu	amphibole peridotite, olivine/amphibole pyroxenite, (hornblende) gabbro
Hadong	0.70×0.3	0.15	in exploration	olivine/amphibole pyroxenite, gabbro
Mati	0.45×0.2	0.07	in exploration	amphibole peridotite, olivine/amphibole pyroxenite, hornblende gabbro
Hulu	1.81×0.41	0.62	medium-sized Ni-Cu	amphibole peridotite, olivine/amphibole pyroxenite, hornblende gabbro, diorite
Huangshan	3.8×0.8	1.71	Large Ni-Cu	gabbro-diorite, hornblende-gabbro, hornblende-gabbro-norite, hornblende-lherzolite, hornblende-websterite
Huangshandong	5.3×1.12	2.8	Large Ni-Cu	hornblende-olivine-gabbro,pyroxene-hornblende-gabbro,gabbro diorite, gabbronorite, olivine-gabbro-norite,pyroxene-cortlandtite
Xiangshan	10×0.35	2.5	medium-sized Ni-Cu and Ti-Fe	(amphibole) peridotite, olivine/amphibole pyroxenite, hornblende gabbro, diorite

mounted in epoxy. The mount was then polished, vacuum coated with high-purity gold and photographed in transmitted and reflected light as well as cathodoluminescence (CL) to identify analyzed grains. Measurements of U, Th and Pb were conducted using the Cameca IMS-1280 SIMS at the Institute of Geology and Geophysics, Chinese Academy of Sciences in Beijing. U-Th-Pb ratios and absolute abundances were determined relative to the standard zircon TEMORA, analyses of which were interspersed with those of unknown grains, using operating and data processing procedures similar to those described by Li and others (2009). A long-term uncertainty of 1.5 percent (1 RSD) for $^{206}Pb/^{238}U$ measurements of the standard zircons was propagated to the unknowns (Li and others, 2010), despite that the measured $^{206}Pb/^{238}U$ error in a specific session is generally around 1 percent (1 RSD) or less. Measured compositions were corrected for common Pb using non-radiogenic ^{204}Pb. Corrections are sufficiently small to be insensitive to the choice of common Pb composition, and an average of present-day crustal composition (Stacey and Kramers, 1975) is used for the common Pb assuming that the common Pb is largely surface contamination introduced during sample preparation. Uncertainties on individual analyses in data tables are reported at a 1 σ level; mean ages for pooled U/Pb (and Pb/Pb) analyses are quoted with 95 percent confidence interval. Data reduction was carried out using the Isoplot/Ex v. 2.49 program (Ludwig, 2001). Zircon U-Th-Pb isotopic data are presented in table 2 and illustrated in figure 3.

ANALYTICAL RESULTS AND COMPILED DATASET

Zircon grains from all samples are transparent and mostly euhedral to subhedral and 30 to 150 μm in length, with some exhibiting concentric zoning. 15 grains from the Poshi gabbro (PSZK1-2-650) were analyzed (table 2). U, Th and Pb contents of the Poshi zircons vary from 124 to 302 ppm, 109 to 350 ppm and 7.36 to 18.7 ppm, respectively, and Th/U ratios are *ca.* 0.70~1.24. All analyses have concordant U-Pb ages within analytical errors (fig. 3), yielding a concordia age of 284.0 ± 2.2 Ma (MSWD = 0.94). 11 zircon grains from the Hongshishan diorite (HSS12) have large variations in U, Th and Pb contents of 210~1536 ppm, 114~1412 ppm, and 11.4~90.6 ppm respectively, and Th/U ratios of 0.54~1.16, yielding a mean $^{206}Pb/^{238}U$ age of 279.7 ± 4.8 Ma (MSWD = 3) (fig. 3). The zircons from the rhyolite sample (HSS6) have U contents in the range of 186~813 ppm, Th of 90~863 ppm, Pb of 10.0~50.7 ppm, Th/U ratios of 0.48~1.06, and a concordia age of 279.1 ± 2.9 Ma (MSWD = 0.25) (fig. 3). Thirteen analyses of the Bijiashan gabbroic zircons show that U, Th, Pb and Th/U have ranges of 267~2827 ppm, 164~2271 ppm, 15.0~171 ppm and 1.29~1.49, respectively, and a concordia age of 279.2 ± 2.3 Ma (MSWD = 2.6) (fig. 3). The analyzed 22 zircon grains from the Xianghshan gabbro (XSTiFe-V) yielded a concordia age of 278.6 ± 1.8 Ma (MSWD = 1.2) (fig. 3) with U contents of 29~158 ppm, Th of 11~110 ppm, Pb of 1.6~8.8 ppm, and Th/U ratios of 0.27~0.70. Six analyses were done on the Huangshan gabbroic zircons and yielded a concordia age of 283.8 ± 3.4 Ma (MSWD = 0.001) (fig. 3) and relatively restricted U, Th, Pb and Th/U variations (table 2).

We also compiled the published and some unpublished age data of basalts in the Tarim basin and mafic-ultramafic intrusions in the Eastern Tianshan and Beishan Rift for comparison and statistical purposes. Although a great number of the age data obtained by different analytical methods have been published, only the data measured by more precise analytical methods were used. For example, K-Ar, ^{39}Ar-^{40}Ar age, zircon LA-ICP-MS and SHRIMP U-Pb ages on basalts are included, and TIMS, LA-ICP-MS, SHRIMP and SIMS zircon U-Pb ages on mafic-ultramafic intrusions are compiled in this study (table 3; fig. 4). The compiled Sr-Nd isotopic data of basalts and mafic-ultramafic intrusions are listed in table 4 and recalculated back to initial ratios corresponding to their ages illustrated in figure 5. Data sources are listed in table 4.

Table 2

U-Pb age determined by SIMS of zircons separated from mafic-ultramafic intrusions in the Eastern Tianshan and Beishan

sample/spot	U ppm	Th ppm	Pb ppm	Th/U	$^{207}Pb/^{235}U$	±σ %	$^{206}Pb/^{238}U$	±σ %	$^{207}Pb/^{206}Pb$	±σ %	$t_{207/206}$ Ma	±σ	$t_{207/235}$ Ma	±σ	$t_{206/238}$ Ma	±σ
Poshi																
PSZK1-2-650@1	266	190	15.3	0.71	0.320	2.15	0.045	1.50	0.052	1.54	264.1	35.0	281.9	5.3	284.1	4.2
PSZK1-2-650@2	183	164	11.1	0.89	0.332	2.37	0.045	1.51	0.053	1.83	340.0	41.0	291.1	6.0	285.0	4.2
PSZK1-2-650@3	291	340	18.7	1.17	0.322	2.19	0.045	1.51	0.052	1.58	264.5	35.9	283.5	5.4	285.8	4.2
PSZK1-2-650@4	227	281	14.7	1.24	0.316	2.38	0.043	1.51	0.051	1.84	250.3	41.7	279.1	5.8	282.6	4.2
PSZK1-2-650@5	124	109	7.36	0.88	0.314	3.78	0.044	1.52	0.051	3.46	229.8	78.1	277.3	9.2	283.0	4.2
PSZK1-2-650@6	302	350	19.3	1.16	0.318	2.09	0.045	1.50	0.051	1.45	239.5	33.1	280.7	5.1	285.6	4.2
PSZK1-2-650@7	267	302	17.1	1.13	0.321	2.16	0.046	1.52	0.051	1.53	245.7	35.0	282.7	5.3	287.2	4.3
PSZK1-2-650@8	215	183	12.9	0.85	0.324	2.27	0.042	1.50	0.052	1.70	303.1	38.2	285.0	5.6	282.8	4.2
PSZK1-2-650@9	265	185	15.2	0.70	0.320	2.24	0.043	1.50	0.052	1.66	266.9	37.7	281.9	5.5	283.7	4.2
PSZK1-2-650@10	284	333	18.0	1.17	0.324	2.11	0.044	1.50	0.053	1.48	324.4	33.3	285.2	5.3	280.4	4.1
PSZK1-2-650@11	230	238	14.2	1.04	0.329	2.82	0.043	1.51	0.053	2.38	332.4	53.1	288.6	7.1	283.2	4.2
PSZK1-2-650@12	286	339	18.5	1.18	0.324	2.11	0.046	1.50	0.052	1.49	265.1	33.8	285.0	5.3	287.4	4.2
PSZK1-2-650@13	221	241	13.8	1.09	0.319	2.42	0.044	1.51	0.052	1.89	291.8	42.6	281.5	6.0	280.3	4.1
PSZK1-2-650@14	175	189	11.1	1.08	0.323	2.41	0.045	1.51	0.052	1.88	264.8	42.5	284.1	6.0	286.4	4.2
PSZK1-2-650@15	261	289	16.7	1.11	0.320	2.17	0.045	1.51	0.051	1.56	250.1	35.5	281.7	5.3	285.5	4.2
Hongshishan																
HSS12@1	1536	1389	90.6	0.90	0.308	2.37	0.044	1.50	0.051	1.83	229.9	41.8	272.3	5.7	277.2	4.1
HSS12@2	1066	1238	68.3	1.16	0.323	1.78	0.045	1.50	0.052	0.95	272.7	21.7	284.0	4.4	285.4	4.2
HSS12@3	210	114	11.4	0.54	0.337	2.51	0.044	1.52	0.055	2.01	415.0	44.2	294.8	6.5	279.9	4.2
HSS12@4	431	411	25.9	0.95	0.320	2.23	0.042	1.50	0.052	1.65	286.7	37.4	281.6	5.5	281.0	4.1
HSS12@5	396	232	21.9	0.59	0.304	2.22	0.045	1.51	0.049	1.63	143.5	37.8	269.1	5.3	283.8	4.2
HSS12@6	954	947	59.1	0.99	0.333	1.93	0.045	1.50	0.053	1.21	338.3	27.1	291.9	4.9	286.2	4.2
HSS12@7	434	303	23.1	0.70	0.295	2.18	0.042	1.51	0.051	1.57	234.4	35.9	262.5	5.1	265.7	3.9
HSS12@8	1254	1412	77.2	1.13	0.318	1.78	0.044	1.51	0.053	0.93	313.3	21.0	280.1	4.4	276.2	4.1
HSS12@9	398	279	22.4	0.70	0.310	2.32	0.044	1.50	0.051	1.77	221.1	40.5	273.8	5.6	280.0	4.1
HSS12@10	765	740	44.3	0.97	0.317	2.30	0.043	1.51	0.053	1.74	335.2	38.9	279.6	5.6	273.0	4.0
HSS12@11	909	744	54.8	0.82	0.335	2.07	0.046	1.52	0.052	1.41	304.9	31.9	293.4	5.3	292.0	4.3

TABLE 2
(continued)

sample/spot	U ppm	Th ppm	Pb ppm	Th/U	$^{207}Pb/^{235}U$	±σ %	$^{206}Pb/^{238}U$	±σ %	$^{207}Pb/^{206}Pb$	±σ %	$t_{207/206}$ Ma	±σ	$t_{207/235}$ Ma	±σ	$t_{206/238}$ Ma	±σ
Hongshishan																
HSS6@1	225	123	12.0	0.55	0.304	2.49	0.044	1.50	0.050	1.98	217.6	45.3	269.2	5.9	275.2	4.0
HSS6@2	636	555	37.8	0.87	0.314	2.14	0.045	1.50	0.051	1.52	220.8	34.8	277.8	5.2	284.6	4.2
HSS6@3	724	618	41.5	0.85	0.307	1.90	0.043	1.50	0.051	1.16	254.7	26.3	271.9	4.5	274.0	4.0
HSS6@4	484	485	28.9	1.00	0.314	2.09	0.044	1.50	0.052	1.45	290.8	32.9	277.4	5.1	275.8	4.1
HSS6@5	186	90	10.0	0.48	0.324	2.93	0.041	1.64	0.052	2.43	302.8	54.4	284.6	7.3	282.4	4.5
HSS6@6	813	863	50.7	1.06	0.330	2.21	0.045	1.52	0.053	1.60	330.4	36.0	289.3	5.6	284.3	4.2
HSS6@7	346	237	19.2	0.68	0.312	2.34	0.044	1.51	0.051	1.78	262.0	40.4	275.7	5.7	277.3	4.1
HSS6@8	659	503	38.1	0.76	0.323	1.90	0.044	1.50	0.052	1.16	302.6	26.3	284.5	4.7	282.3	4.1
Bijiashan																
BJS-6@1	789	413	41.8	0.52	0.311	2.21	0.044	1.50	0.052	1.62	271.3	36.7	275.0	5.3	275.5	4.1
BJS-6@2	867	1014	55.9	1.17	0.322	1.97	0.042	1.50	0.052	1.28	304.0	28.9	283.8	4.9	281.3	4.1
BJS-6@3	397	271	21.9	0.68	0.310	3.13	0.044	1.52	0.051	2.74	247.8	61.8	273.8	7.5	276.9	4.1
BJS-6@4	698	424	38.1	0.61	0.309	2.29	0.044	1.51	0.051	1.72	256.6	39.1	273.4	5.5	275.4	4.1
BJS-6@5	1050	305	53.2	0.29	0.313	1.97	0.043	1.50	0.051	1.27	234.9	29.1	276.2	4.8	281.1	4.1
BJS-6@6	1563	2208	104	1.41	0.312	1.99	0.043	1.50	0.052	1.31	303.4	29.5	275.8	4.8	272.6	4.0
BJS-6@7	493	306	28.0	0.62	0.323	2.02	0.045	1.50	0.052	1.36	282.0	30.7	284.0	5.0	284.3	4.2
BJS-6@8	2827	2271	171	0.80	0.328	1.61	0.046	1.50	0.051	0.56	257.8	12.9	288.4	4.0	292.2	4.3
BJS-6@9	2471	2195	148	0.89	0.324	1.74	0.043	1.50	0.052	0.88	297.3	20.0	284.6	4.3	283.1	4.2
BJS-6@10	485	416	27.7	0.86	0.299	2.19	0.043	1.50	0.050	1.59	210.5	36.4	265.8	5.1	272.1	4.0
BJS-6@11	267	164	15.0	0.61	0.318	2.38	0.042	1.51	0.051	1.84	262.2	41.6	280.5	5.8	282.6	4.2
BJS-6@12	915	1360	62.4	1.49	0.314	1.99	0.044	1.50	0.051	1.30	239.9	29.7	277.1	4.8	281.6	4.1
BJS-6@13	2025	905	107	0.45	0.313	2.62	0.044	1.51	0.052	2.14	266.3	48.4	276.6	6.4	277.9	4.1
Xiangshan																
XSTiFe@1	60	32	3.2	0.53	0.323	3.68	0.044	1.55	0.053	3.34	348.4	73.7	284.3	9.2	276.5	4.2
XSTiFe@2	80	44	4.4	0.55	0.321	2.55	0.044	1.50	0.052	2.06	280.7	46.6	283.0	6.3	283.3	4.2
XSTiFe@3	86	45	4.7	0.52	0.309	2.76	0.044	1.50	0.050	2.32	203.8	52.9	273.7	6.6	282.0	4.1
XSTiFe@4	29	11	1.6	0.36	0.321	4.09	0.046	1.67	0.051	3.74	241.3	83.9	282.8	10.2	287.8	4.7
XSTiFe@5	100	55	5.4	0.55	0.320	2.40	0.044	1.50	0.052	1.88	299.8	42.2	282.2	5.9	280.1	4.1
XSTiFe@6	130	91	7.3	0.70	0.317	2.24	0.044	1.52	0.052	1.65	288.2	37.3	279.4	5.5	278.3	4.1

Table 2
(continued)

sample/spot	U ppm	Th ppm	Pb ppm	Th/U	$^{207}Pb/^{235}U$	±σ %	$^{206}Pb/^{238}U$	±σ %	$^{207}Pb/^{206}Pb$	±σ %	$t_{207/206}$ Ma	±σ	$t_{207/235}$ Ma	±σ	$t_{206/238}$ Ma	±σ
Xiangshan																
XSTiFe@7	73	40	4.0	0.55	0.321	3.52	0.042	1.64	0.052	3.11	288.2	69.5	282.3	8.7	281.6	4.5
XSTiFe@8	71	34	3.7	0.47	0.322	3.28	0.043	1.56	0.055	2.89	401.1	63.4	283.6	8.1	269.5	4.1
XSTiFe@9	81	45	4.5	0.56	0.332	2.66	0.043	1.66	0.054	2.08	354.3	46.2	291.4	6.8	283.7	4.6
XSTiFe@10	98	55	5.3	0.56	0.307	2.92	0.044	1.52	0.050	2.49	200.9	56.8	271.7	7.0	280.0	4.2
XSTiFe@11	61	33	3.4	0.54	0.340	2.88	0.046	1.63	0.054	2.37	379.3	52.5	297.4	7.4	287.0	4.6
XSTiFe@12	102	57	5.5	0.55	0.320	2.95	0.044	1.54	0.053	2.51	323.8	56.0	281.6	7.3	276.6	4.2
XSTiFe@13	117	70	6.4	0.60	0.321	2.91	0.044	1.57	0.053	2.45	317.0	54.8	282.6	7.2	278.5	4.3
XSTiFe@14	99	64	5.5	0.65	0.320	2.43	0.044	1.51	0.053	1.91	323.0	42.7	281.8	6.0	276.8	4.1
XSTiFe@15	100	58	5.4	0.58	0.316	3.31	0.044	1.52	0.053	2.94	311.1	65.7	279.0	8.1	275.1	4.1
XSTiFe@16	108	63	5.9	0.58	0.313	2.60	0.044	1.53	0.052	2.10	275.9	47.3	276.3	6.3	276.3	4.2
XSTiFe@17	70	39	3.7	0.55	0.293	3.57	0.044	1.52	0.049	3.24	142.1	74.2	261.1	8.3	274.5	4.1
XSTiFe@18	158	110	8.8	0.69	0.327	2.75	0.044	1.51	0.054	2.30	366.9	51.0	286.9	6.9	277.2	4.1
XSTiFe@19	114	31	5.7	0.27	0.308	2.58	0.044	1.53	0.051	2.08	233.1	47.3	272.4	6.2	276.9	4.2
XSTiFe@20	80	44	4.3	0.54	0.311	2.64	0.044	1.51	0.051	2.17	259.0	49.1	275.0	6.4	276.9	4.1
XSTiFe@21	66	32	3.5	0.49	0.309	2.87	0.044	1.56	0.051	2.41	246.7	54.6	273.6	6.9	276.8	4.2
XSTiFe@22	98	52	5.3	0.53	0.321	2.69	0.044	1.51	0.053	2.23	317.8	49.9	282.6	6.7	278.4	4.1
Huangshan																
HS-V@1	553	374	31.4	0.68	0.320	1.85	0.042	1.50	0.052	1.07	280.5	24.4	281.8	4.6	281.9	4.1
HS-V@2	189	111	10.5	0.59	0.316	3.04	0.044	1.51	0.051	2.64	254.4	59.6	279.1	7.5	282.1	4.2
HS-V@3	445	346	25.7	0.78	0.313	1.93	0.044	1.50	0.051	1.22	234.5	27.9	276.4	4.7	281.3	4.1
HS-V@4	920	763	54.6	0.83	0.328	1.72	0.045	1.50	0.053	0.84	309.7	19.0	288.2	4.3	285.6	4.2
HS-V@5	224	138	12.5	0.62	0.329	2.49	0.044	1.51	0.053	1.98	337.2	44.2	289.2	6.3	283.3	4.2
HS-V@6	423	305	24.8	0.72	0.323	2.75	0.046	1.50	0.051	2.31	238.4	52.3	284.1	6.8	289.6	4.3

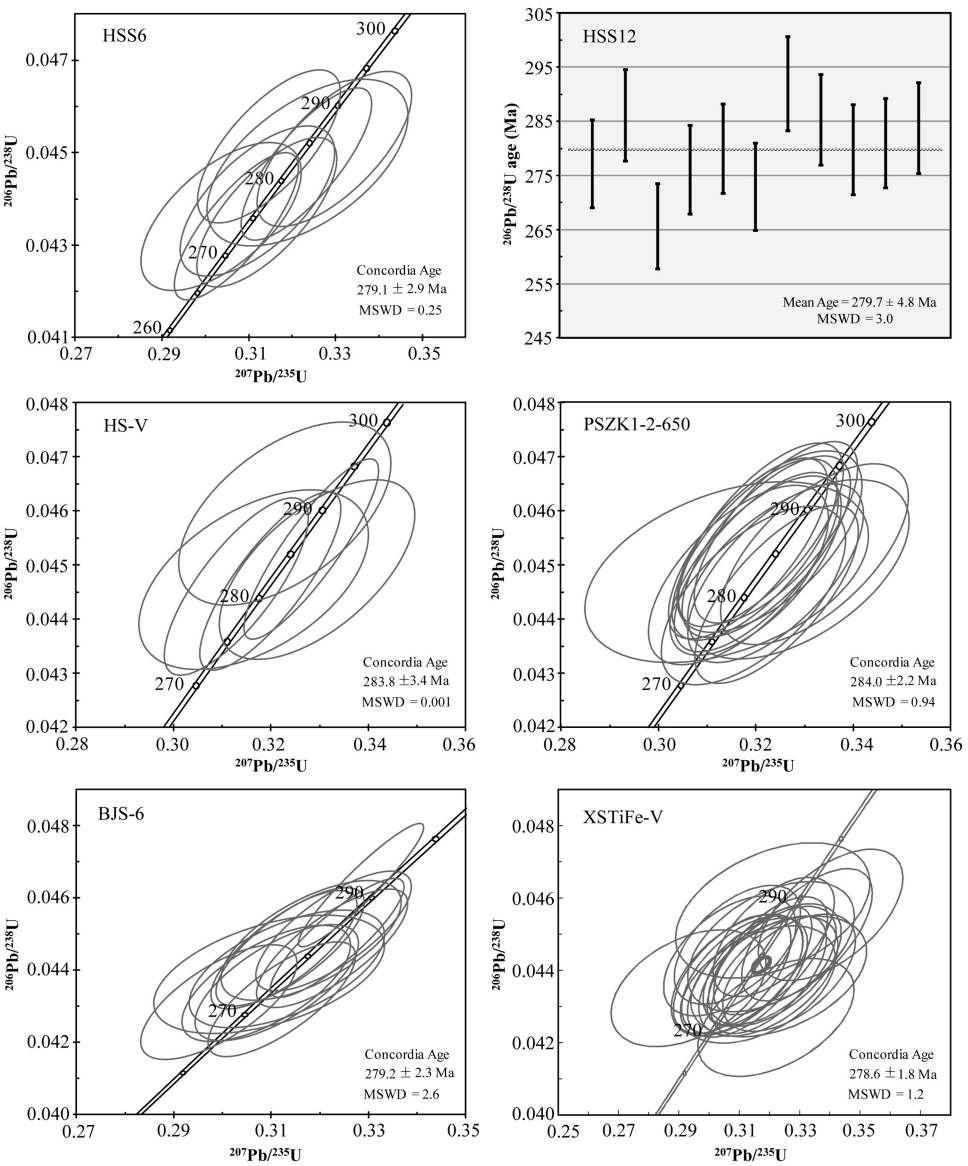

Fig. 3. U-Pb concordia plots showing zircon SIMS analytical data of Hongshishan dacite and diorite, Huangshan gabbro, Poshi gabbro, Bijiashan gabbro and Xiangshan gabbro.

The data sources of whole rock TiO_2 and Mg# (Mg# = Mg/(Mg+Fe)×100) are listed in the figure caption for figure 6.

DISCUSSION

Proposed Possible Early-Permian Mantle Plume in NW China

Early-Permian eruptive and intrusive rocks in NW China are widespread, particularly in Tianshan and its adjacent regions. Basalts are mainly distributed in the Tarim

Basin and sporadically along the Tianshan Mountains (Jia and others, 1995; Chen and others, 1997; Zhang and others, 2003; Xia and others, 2003, 2006; Yang and others, 2005, 2006; Li and others, 2007, 2008; Zhou and others, 2009). Most of the Permian basalts in the Eastern Tianshan and Beishan should have been eroded away because the Kangguer-Huangshan ductile shear zone hosting Carboniferous volcanic rocks and tuff, and ductile shear belt type gold deposits are cropping out at the surface at present (Qin and others, 2002a, 2003). Minor amounts of basalts present in the Eastern Tianshan and Beishan Rift may represent relicts (Mao and others, 2008; Pirajno and others, 2008; Xu and others, 2009). Large volumes of intermediate-acidic volcanic successions and associated granitic rocks were erupted/intruded during the Late Carboniferous–Early Permian in NW China (Han and others, 1997; Jahn and others, 2000a, 2000b, 2004; Xia and others, 2003, 2006; Xiao and others, 2004b, 2009; Wang and others, 2009; Su and others, 2010a). Their distribution has been identified as a large igneous province (LIP) in NW China (Xia and others, 2003, 2006; Yang and others, 2007; Chen and others, 2009; Zhou and others, 2009). These volcanic rocks have oceanic island basalt (OIB)-like geochemical features (Xia and others, 2003, 2006 and references therein; Zhou and others, 2009) and the granites are characterized by positive $\varepsilon_{Nd}(t)$ (Jahn and others, 2000a, 2000b, 2004; Wang and others, 2009 and references therein), suggesting a large scale underplating of mantle derived magmas beneath the crust in NW China during the Early Permian. Furthermore, the mafic/ultramafic intrusive dikes and sills outcropping in the Eastern Tianshan, Beishan Rift and the margin of the Tarim LIP, have features of low Ti and estimated high-Mg parental magmas (generally >12 wt.%), which require very high mantle temperatures estimated to be in the range of 1100~1600 °C using equilibrium mineral assemblages (Zhang and others, 2003; Zhou and others, 2004; Yang and others, 2007b; Chai and others, 2008; Mao and others, 2008; Pirajno and others, 2008; Su and others, 2009; Sun and others, 2009; Tang and others, 2009) consistent with the experimental modeled temperatures (Nisbet and others, 1993; Herzberg and O'Hara, 2002; Isley and Abbott, 2002). Additionally, Mao and others (2006b, 2008) suggested that these mafic-ultramafic intrusions might be the root of the erupted basalts, which were eroded away in the Eastern Tianshan and Beishan Rift, and subsequently preserved in the Tarim Basin.

Recently, Tian and others (2010) reported major and trace element composition, Sr-Nd isotopic and seismological data for a picrite-basalt-rhyolite suite from the northern Tarim uplift. They studied samples from 13 boreholes at depths between 5,166 and 6,333 m. The picrite samples have high MgO (14.5~16.8 wt.%, volatiles included) and are enriched in incompatible element and have high $^{87}Sr/^{86}Sr$ (Sr_i = 0.707) and low $^{143}Nd/^{144}Nd$ isotopic ratios [$\varepsilon_{Nd}(t)$ down to −5.3], resembling the Karoo high-Ti picrites. The picrite-basalt-rhyolite suite, together with Permian volcanic rocks from elsewhere in the Tarim Basin, constitute a LIP that is characterized by a large areal extent, rapid eruption, OIB-type chemical composition, and eruption of high temperature picritic magma.

The above observations and geochemical features have been attributed to activities of mantle plume (Xia and others, 2003, 2004; Zhou and others, 2004; Yang and others, 2007a, 2007b; Mao and others, 2008; Pirajno and others, 2008; Chen and others, 2009), which may be correlated with global plume activities such as the ~251 Ma Siberian and ~260 Ma Emeishan plumes (fig. 1) in the Permian. Although a possible mantle plume could be inferred to have initiated magmatic activities in NW China, there is still a lack of exact and adequate evidences to support this, since the identification of an ancient plume is based on uplift prior to volcanism, the orientation of dikes that feed the volcanism, the physical characteristics of the volcanism, the age progression along volcanic chains, and the chemistry of the magmas that mantle

TABLE 3

Compiled ages of basalts and mafic dikes in the Tarim Basin, and mafic-ultramafic intrusions and igneous rocks in the Eastern Tianshan and Beishan

Location	rock type	analytical method	age	error	data source
Tarim Basin volcanic rocks and mafic intrusive rocks					
Sishichang	basalt	K-Ar	292.4	0.5	Jia and others, 1995
Sishichang	basalt	K-Ar	278.0		Chen and others, 1997
Sishichang	basalt	^{39}Ar-^{40}Ar	278.5	1.4	Chen and others, 1997
Yingan	basalt	K-Ar	289.0	6.1	Zhang and others, 2003
Yingan	basalt	^{39}Ar-^{40}Ar	281.8	4.2	Yang and others, 2006
Yingan	basalt	K-Ar	272.9	4.0	Zhang and others, 2003
Yingan	basalt	K-Ar	288.4	4.4	Zhang and others, 2003
Yingan	basalt	K-Ar	287.2	5.6	Yang and others, 2005
Keping	basalt	zircon LA-ICP-MS	275.0	13.0	Li and others, 2007
Keping	basalt	zircon SHRIMP	279.0	4.5	Chen and others, 2010
Taxinan	basalt	K-Ar	289.6	5.6	Li and others, 2008
Taxinan	basalt	^{39}Ar-^{40}Ar	290.1	3.5	Yang and others, 2006
Tashen	basalt	K-Ar	282.7	4.1	Yang and others, 2006
Yingmai	basalt	K-Ar	290.5	4.2	Yang and others, 2006
Keping	volcanic tuff	zircon LA-ICP-MS	291.0	10.0	Li and others, 2007
Keping	gabbro	zircon LA-ICP-MS	274.0	15.0	Li and others, 2007
Xiaohaizi	diabase	zircon LA-ICP-MS	272.0	6.0	Li and others, 2007
Tahe	volcanic rock	zircon SHRIMP	276.0	3.0	Yang and others, 2006
Kuche	rhyolite	^{39}Ar-^{40}Ar	278.0	1.3	Chen and others, 1998
Bachu	quartz syenite	zircon LA-ICP-MS	274.0	2.0	Zhang and others, 2008
Bachu	quartz syenite	zircon SHRIMP	273.0	3.7	Chen and others, 2010
Yingmai	syenite	K-Ar	287.6	2.8	Chen and others, 1999
Xiaohaizi	syenite	^{39}Ar-^{40}Ar	277.7	1.3	Yang and others, 1996
Xiaohaizi	syenite	zircon SHRIMP	277.0	4.0	Yang and others, 2007
Xiaohaizi	syenite	zircon LA-ICP-MS	282.0	3.0	Li and others, 2007
Xiaohaizi	syenite	zircon LA-ICP-MS	281.0	4.0	Li and others, 2007
Yingmai	rhyolite	zircon LA-ICP-MS	271.7	2.2	Tian and others, 2010
Yingmai	rhyolite	zircon SHRIMP	277.3	2.5	Tian and others, 2010
Yingmai	rhyolite	zircon LA-ICP-MS	282.9	2.5	Tian and others, 2010
Yingmai	rhyolite	zircon LA-ICP-MS	290.1	3.5	Tian and others, 2010
Yingmai	basalt	zircon LA-ICP-MS	286.6	3.3	Tian and others, 2010
Tashen	basalt	^{39}Ar-^{40}Ar	268.9	4.2	Zhang and others, 2010
Tashen	basalt	^{39}Ar-^{40}Ar	271.1	3.5	Zhang and others, 2010
Xiaohaizi	basalt	^{39}Ar-^{40}Ar	285.4	8.5	Zhang and others, 2010
Bachu	basalt	^{39}Ar-^{40}Ar	273.0	13.5	Zhang and others, 2010
Keping	basalt	^{39}Ar-^{40}Ar	276.8	3.4	Zhang and others, 2010
Keping	basalt	^{39}Ar-^{40}Ar	273.8	6.3	Zhang and others, 2010
Keping	basalt	^{39}Ar-^{40}Ar	282.9	1.6	Zhang and others, 2010
Eastern Tianshan and Beishan mafic-ultramafic complexes and igneous rocks					
Xuanwoling	gabbro	zircon SIMS	260.7	2.0	Su and others, 2010a
Poshi	hornblende gabbro	zircon TIMS	274.0	4.0	Jiang and others, 2006
Poshi	gabbro	zircon SHRIMP	278.0	2.0	Li and others, 2006a
Poshi	olivine gabbro	zircon SIMS	275.5	1.2	Ao, 2010
Poshi	olivine gabbro	zircon SIMS	284.0	2.2	this study
Poyi	alkaline granite vein	zircon SIMS	251.4	1.8	Su and others, 2010b
Poyi	gabbro	zircon SIMS	271.0	6.2	Ao, 2010
Luodong	gabbro	zircon SIMS	284.0	2.3	Su and others, 2010b
Luodong	gabbro	zircon LA-ICP-MS	283.8	1.1	Ao, 2010
Hongshishan	olivine gabbro	zircon LA-ICP-MS	281.8	2.6	Ao and others, 2010
Hongshishan	troctolite	zircon SIMS	286.4	2.8	Su and others, 2010c
Hongshishan	diorite	zircon SIMS	279.7	4.8	this study
Hongshishan	dacite	zircon SIMS	279.1	2.9	this study
Bijiashan	gabbro	zircon SIMS	279.2	2.3	this study
Tianyu	gabbro	zircon SIMS	280.0	2.0	Tang and others unpublished
Tianyu	gabbro	zircon LA-ICP-MS	290.2	3.4	Tang and others, 2009

TABLE 3
(continued)

Location	rock type	analytical method	age	error	data source
Eastern Tianshan and Beishan mafic-ultramafic complexes and igneous rocks					
Baishiquan	gabbro	zircon LA-ICP-MS	284.8	5.7	Su and others, 2010b
Baishiquan	gabbro	zircon LA-ICP-MS	281.2	0.9	Mao and others, 2006a
Baishiquan	gabbro	zircon SHRIMP	284.0	8.0	Wu and others, 2005
Baishiquan	diorite	zircon SHRIMP	284.0	9.0	Wu and others, 2005
Baishiquan	quartz diorite	zircon SHRIMP	285.0	10.0	Wu and others, 2005
Huangshan	gabbro	zircon SIMS	283.8	3.4	this study
Huangshanxi	diorite	zircon SHRIMP	269.0	2.0	Zhou and others, 2004
Huangshandong	olivine norite	zircon SHRIMP	274.0	3.0	Han and others, 2004
Xiangshan	gabbro	zircon SIMS	279.6	1.1	Han and others, 2010
Xiangshan	gabbro	zircon SHRIMP	283.0	3.0	Wang and others, 2009
Xiangshan	gabbro	zircon SHRIMP	285.0	1.2	Qin and others, 2002a
Xiangshan	Ti-Fe gabbro	zircon SIMS	278.6	1.8	this study
Hulu	diorite	zircon SHRIMP	274.0	3.9	Xia and others, 2008
Tulaergen	gabbro	zircon SIMS	300.5	3.2	San and others, 2010
Haibaotan	gabbro	zircon SHRIMP	269.2	3.2	Li and others, 2006b
Haibaotan	anorthosite	zircon SHRIMP	284.5	2.5	Li and others, 2006b
Qiatertage	gabbro	zircon SHRIMP	277.0	1.6	Li and others, 2006b

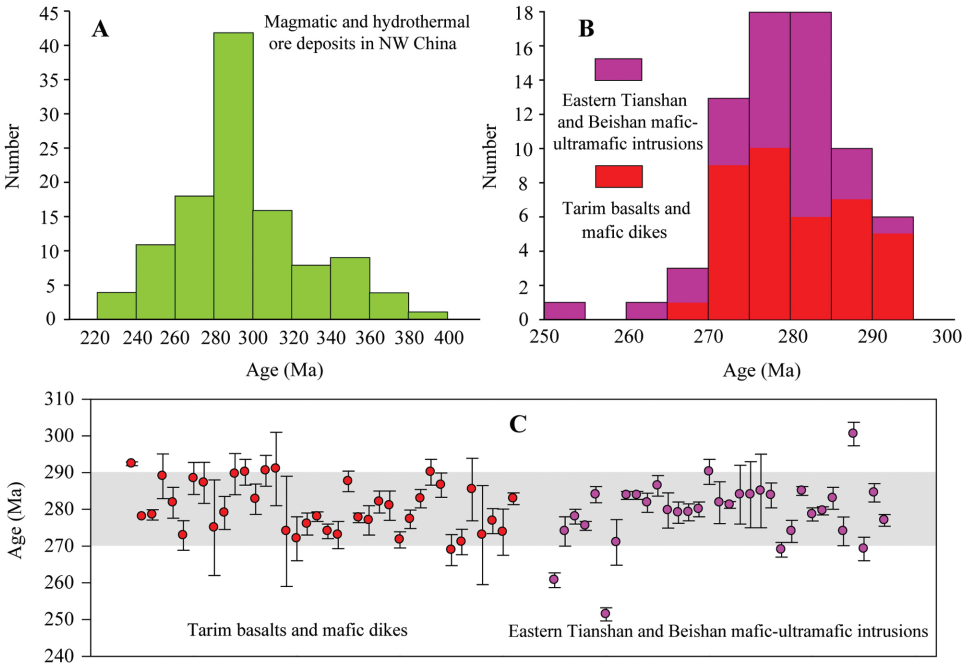

Fig. 4. (A) Histogram of compiled age data (n = 119) of magmatic and hydrothermal ore deposits in NW China yielding a peak age between 280~300 Ma (after Pirajno and others, 2008 and references therein). (B) Histogram of compiled age data (n = 71) of basalts and mafic/ultramafic dikes/intrusions in Tarim Basin, Eastern Tianshan and Beishan (data sources: see table 2). (C) Compiled ages with errors showing a *ca.* 280 Ma peak.

TABLE 4

Compiled Sr-Nd isotopes of basalts and mafic dykes in the Tarim Basin, and mafic-ultramafic intrusions and igneous rocks in the Eastern Tianshan and Beishan

locality	$^{87}Rb/^{86}Sr$	$^{87}Sr/^{86}Sr$	$(^{87}Sr/^{86}Sr)i$	$^{147}Sm/^{144}Nd$	$^{143}Nd/^{144}Nd$	$(^{143}Nd/^{144}Nd)i$	$\varepsilon_{Nd}(t)$	data source
Eastern Tianshan and Beishan mafic-ulatramafic intrusion								
Pobei	0.024600~0.672000	0.705065~0.708367	0.704804~0.708271	0.147400~0.223600	0.512522~0.512898	0.512219~0.512358	-1.3~6.8	Jiang and others, 2006
Luodong	0.013180~0.146510	0.703520~0.704240	0.702949~0.704098	0.195880~0.225760	0.513010~0.513260	0.512609~0.512843	6.6~11.2	Sun and others, 2010
Hongshishan	0.034262~2.054056	0.704457~0.714581	0.703509~0.707291	0.137281~0.264500	0.512656~0.513050	0.512331~0.512656	1.2~7.6	Su and others, 2010c
Tianyu	0.054578~9.490405	0.705887~0.741586	0.703852~0.708529	0.092173~0.175069	0.512417~0.512764	0.512219~0.512515	-1.1~4.7	Tang and others, 2009
Baishiquan	0.029800~0.956900	0.704005~0.706532	0.703868~0.706241	0.124100~0.157700	0.512613~0.512955	0.512360~0.512665	1.7~7.6	Chai and others, 2008
Huangshanxi	0.016083~0.445950	0.703198~0.705330	0.702498~0.705269	0.139200~0.190000	0.512937~0.513069	0.512633~0.512764	6.7~9.3	Zhou and others, 2004
Huangshandong	0.018264~0.182419	0.703157~0.704788	0.702756~0.704078	0.156000~0.182800	0.512935~0.513068	0.512631~0.512761	6.8~9.3	Zhou and others, 2004
Hulu	0.028480~0.251930	0.703850~0.705030	0.703739~0.704718	0.145600~0.163400	0.512873~0.513000	0.512612~0.512711	6.4~8.3	Xia and others, 2008; Sun and others, 2009
Tulaergen	0.038490~1.791610	0.703990~0.710400	0.702768~0.704680	0.111280~0.177450	0.512280~0.513080	0.512410~0.512732	3.1~9.4	Sun, 2009
Chuanzhu	0.014000~0.115000	0.704000~0.706000	0.703553~0.705673	0.142000~0.185500	0.512900~0.513000	0.512645~0.512726	7.1~8.6	Sun, 2009
Mati	0.007680~0.015580	0.703560~0.703640	0.703530~0.703600	0.180460~0.205500	0.513010~0.513120	0.512674~0.512751	7.6~9.1	Sun, 2009
Tarim Basin mafic dike								
Bachu	0.072000~1.204000	0.703796~0.757022	0.703520~0.706500	0.103400~0.125100	0.512523~0.512620	0.512299~0.512430	0.3~2.8	Zhang and others, 2008
Bachu and Keping basalt	0.115900~0.188200	0.705329~0.705605	0.704818~0.705152	0.123700~0.140600	0.512606~0.512771	0.512369~0.512548	1.7~5.2	Zhou and others, 2009
Bachu and Keping	0.045000~0.177100	0.707017~0.708647	0.706386~0.708034	0.127000~0.136400	0.512055~0.512388	0.511891~0.512148	-9.2~-2.6	Zhou and others, 2009
Keping		0.707483~0.709284	0.706104~0.708183		0.512322~0.512416		-3.7~-1.7	Jiang and others, 2004

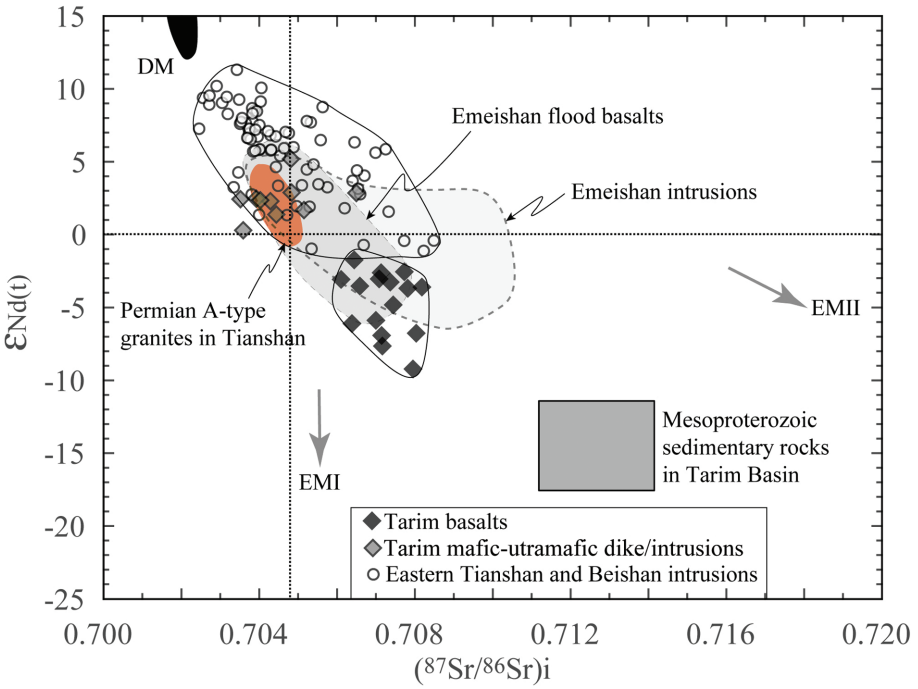

Fig. 5. $\varepsilon_{Nd(t)}$ versus $(^{87}Sr/^{86}Sr)_i$ plot of Sr and Nd isotopic compositions of basalts and mafic/ultramafic dykes/intrusions in Tarim Basin, Eastern Tianshan and Beishan (data sources: see table 3). DM (depleted mantle) and EM (enriched mantle) are from Zindler and Hart (1986). Fields of the Emeishan flood basalts and intrusions are from Zhou and others (2008). Mesoproterozoic sedimentary rocks in Tarim and Permian A-type granites in Tianshan fields are from Zhang and others (2008) and references therein.

plumes produce (Condie, 2001; Ernst and Buchan, 2003). Some fundamental geochronological and geochemical constraints are offered in the discussion below.

Geochronological Constraints

Some geochronological constraints on a possible mantle plume have been done by Pirajno and others (2008) and Zhang and others (2008). The mineralization ages of 119 magmatic and hydrothermal ore deposits in NW China (fig. 3A) compiled by Pirajno and others (2008) range from 250 to 320 Ma with the peak at 280~300 Ma. This was assumed to be the time when the mantle plume was mostly active. Compiled age data of 18 mafic and 21 granitic rocks by Zhang and others (2008) gave a similar age span of 260~320 Ma but a different peak of 275 Ma, which was interpreted to represent the plume age. Since flood basalts have genetic affinity to mafic-ultramafic intrusions such as in the Emeishan mantle plume region (Condie, 2001; Isley and Abbott, 2002; Ernst and Buchan, 2003; Xiao and others, 2003, 2004a; Zhong and Zhu, 2006; Zhou and others, 2008), the compilation of both age datasets can be used to clarify the issue on the age of the mantle plume.

Up to date published age data of the Tarim basalts and mafic dikes show a wide range between 271 Ma and 292 Ma, including zircon U-Pb age data by LA-ICP-MS and SHRIMP, which have relatively large errors of up to 15 Ma, and K-Ar and ^{39}Ar-^{40}Ar which yield small errors (table 3; fig. 4C). For example, the analysis of basalts from the same locality, by the same method in an individual study generated distinct results (table 3), which might depend on their sampling depth/layer. Thus, a histogram of

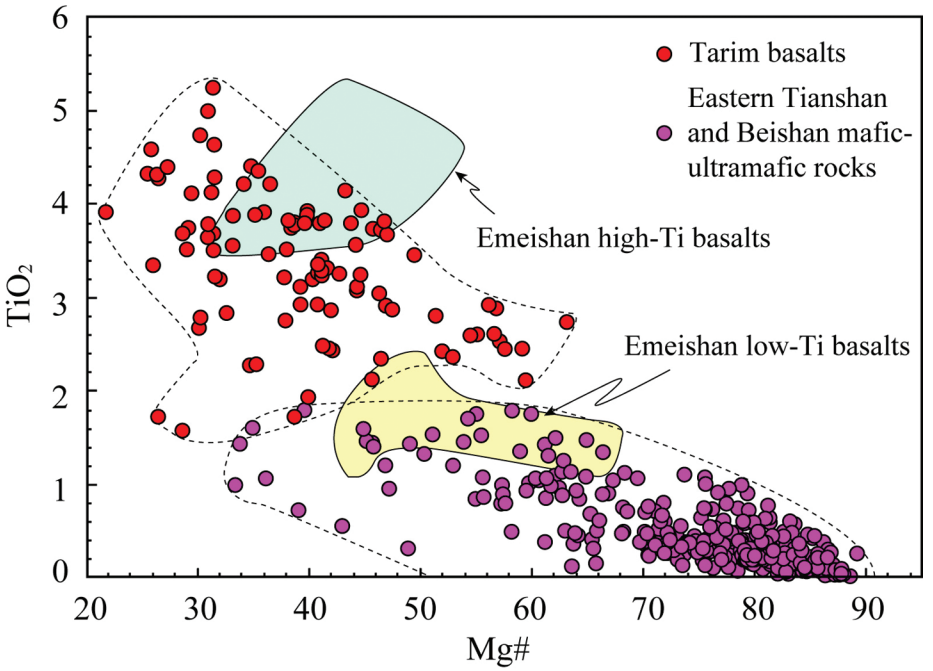

Fig. 6. Whole rock TiO_2 versus Mg# plot of basalts and mafic/ultramafic dykes/intrusions in the Tarim Basin, Eastern Tianshan and Beishan (Data compiled from Chen and others, 1997; Zhou and others, 2004, 2009; Jiang and others, 2004, 2006; Li and others, 2006b; Chai and others, 2008; Li and others, 2008; Xia and others, 2008; Sun and others, 2009; Tang and others, 2009; Xiao and others, 2010; Su and others, 2010c, 2010d; Zhang and others, 2010). Emeishan high-Ti and low-Ti basalts fields are from Xiao and others (2004a).

basalt ages exhibits a flat pattern without any peak (fig. 4B), indicating that it cannot yield the exact constraint on the mantle plume. Zircon U-Pb dating on mafic-ultramafic intrusions by a more precise method using Cameca IMS 1280 in this study yielded a relatively restricted age range between 276.8 Ma and 284.0 Ma (table 3; fig. 3). The compiled zircon U-Pb age data measured by TIMS, SIMS, SHRIMP and LA-ICP-MS illustrate a striking peak with values between 280 Ma and 285 Ma (fig. 4B) and lie within the age range (280~300 Ma) of Pirajno and others (2008) and also within the Tarim basalts age field (272~292 Ma) of Zhang and others (2008). These features imply that the mafic-ultramafic intrusions have a geochronological genetic relation with the basalts. The merged histogram displays a peak of 280 Ma even taking analytical error into account (figs. 4B and 4C), which most likely represents a period of the mantle plume activity in NW China.

A switch from subduction-driven to plume-driven magmatism for the Pacific margin of Gondwanaland during the Mesozoic was suggested to be within 5~10 Myr (Weaver and others, 1994; Storey and others, 1999; Dalziel and others, 2000; Condie, 2001), which could take a little longer in an orogenic belt such as Central Asian Orogenic Belt. The subduction was generally suggested to have ended in the Late-Carboniferous during and before which the subduction-related igneous rocks were well developed in NW China (for example, Jia and others, 1995; Qin and others, 2002b, 2005; Xu and others, 2009). Assuming 295 Ma as the end time of subduction-related magmatism, 280 Ma would therefore be a reasonable age for mantle plume-driven magmatism. Additionally, this mantle plume was taking place in the post-orogenic period.

Sr-Nd Isotopic Constraints

Most OIBs are considered to be the expression of plume tails, whereas continental and oceanic LIPs with chemistry similar to that of OIBs are generally interpreted to represent plume-head events (Campbell and Griffiths, 1990; Saunders and others, 1992, 2005; Chung and Jahn, 1995; Condie, 2001; Ernst and Buchan, 2003). In Sr-Nd isotopic diagrams, oceanic plateaus, which have chemistry similar to OIBs, plot between depleted mantle and chondrite. The radiogenic isotope compositions of continental flood basalts fall outside the range of plume sources defined by OIBs and typically plot within the field of enriched $^{87}Sr/^{86}Sr$ and negative $\varepsilon_{Nd}(t)$, suggesting a possible contamination by lithospheric mantle and continental crust (Campbell and Griffiths, 1990; Ellam and Cox, 1991; Saunders and others, 1992, 2005; Chung and Jahn, 1995; Condie, 2001; Ernst and Buchan, 2003).

The Emeishan flood basalts generated from ~260 Ma mantle plume display very similar geochemical features plotting within the OIB field in Sr-Nd diagram and show lithospheric contamination (table 3; fig. 5; Chung and Jahn, 1995; Xiao and others, 2003, 2004a; Zhou and others, 2008). The Tarim flood basalts have $(^{87}Sr/^{86}Sr)i$ of 0.706104~0.708183 and $\varepsilon_{Nd}(t)$ of −9.2~−1.7 partly overlapping the Emeishan basalts field (table 4; fig. 5). Accordingly, the Tarim basalts have been interpreted to be derived from the asthenosphere and subsequently contaminated by Mesoproterozoic sedimentary rocks during their ascent (fig. 5; Zhang and others, 2008; Zhou and others, 2009). Several studies (for example, Condie, 2001; Ernst and Buchan, 2003; Isley and Abbott, 2002; Zhou and others, 2004) have suggested that mafic-ultramafic intrusions are derived from the lithospheric mantle and have wider compositional ranges due to more extensive contamination. For example, the Emeishan mafic-ultramafic intrusions show larger variations in Sr isotope, although the Nd isotopes are similar to the flood basalts (fig. 5; Zhou and others, 2008). Similarly, the mafic-ultramafic intrusions in the Eastern Tianshan and Beishan Rift have wide Sr-Nd isotope variations in $(^{87}Sr/^{86}Sr)i$ (0.702498~0.708529) and $\varepsilon_{Nd}(t)$ (−1.3~11.2) (table 4) and are correlated with the Tarim basalts (fig. 5). Besides, the mafic dikes close to the Tarim LIPs also show similar isotopic features and mostly plot in the field defined by the mafic-ultramafic intrusions (fig. 5). These features suggest that the flood basalts and mafic-ultramafic intrusions have genetic affinities but distinct magma sources. Furthermore, the plume-related A-type granites are characterized with positive $\varepsilon_{Nd}(t)$ (but usually $< +5$) (Zhong and Xu, 2009). The Permian A-type granites in the Tianshan Mountains have $\varepsilon_{Nd}(t)$ in the range of −1~5 and low $(^{87}Sr/^{86}Sr)i$ of <0.705200 (fig. 5; Zhang and others, 2008). In summary, the OIB-like isotopic compositions and correlated relationship among the flood basalts, mafic-ultramafic intrusions and granites imply that the petrogenesis of these rocks was most likely related to mantle plume activities.

Geochemical Constraints

Mantle plumes can be divided into central/inner, intermediate and outer zones, and igneous rocks in each zone exhibit distinct compositions (Campbell and Griffiths, 1990; Condie, 2001; Ernst and Buchan, 2003; Xiao and others, 2003, 2004a; Saunders and others, 2005; Jourdan and others, 2009). For instance, the basalts of the inner zone of the Emeishan plume are characterized by low TiO_2 contents, whereas high-Ti basalts crop out in the outer zone of the same plume (Xiao and others, 2004a). The explanation for this feature is that Ti as an incompatible element tends to concentrate in low-degree melting magmas rather than high-degree melting magmas linked to high temperatures such as that of mantle plume head (for example, Xu and others, 2001; Xiao and others, 2003, 2004a; Tang and others, 2006). Magmas generated by high-degrees of melting have higher Mg# than the low-degree melting magmas do, and

consequently, TiO_2 content and Mg# of the whole rocks display negative correlations (Herzberg and O'Hara, 2002; Isley and Abbott, 2002; Xiao and others, 2004a). The low-Ti and high-Ti basalts in the Emeishan area display geochemical gaps (fig. 6; Xiao and others, 2004a), and were interpreted to be produced from different source areas: lithospheric mantle and mantle plume (Xiao and others, 2004a). Similar features are present in the southern African LIPs (Jourdan and others, 2009).

The compositions of basalts and mafic-ultramafic rocks in NW China are comparable with the Emeishan basalts and those of the southern African LIPs. The Tarim basalts have high TiO_2 contents of 1.6~5.3 weight percent (mostly >2.2 wt.%) and low Mg# of 22~60 (mostly <50), whereas the Eastern Tianshan and Beishan mafic-ultramafic rocks display low TiO_2 contents (<1.8 wt.%) and large Mg# variations from 33 to 90 (fig. 6). The basalts and the mafic-ultramafic intrusions are likely to correspond to the high-Ti basalts and low-Ti basalts, respectively. Similarly, Xia and others (2003, 2004), on the basis of geochemical data, also suggested that low-Ti lavas are predominantly distributed in the eastern Tianshan rifts and that high-Ti alkaline lavas predominantly erupted in the western Tianshan (Yili rift), and concluded that this spatial variation may be caused by the different thickness of lithosphere and the thermal structure of the asthenospheric mantle. Therefore, the high-Ti and low-Mg basaltic lavas in the western Tianshan and the Tarim Basin may have been produced by lower degrees of melting in the outer zone of the mantle plume characterized by relatively lower temperature and thicker lithosphere, whereas the low-Ti and high-Mg magmas in the Eastern Tianshan and the Beishan Rift were probably generated from the axis of the mantle plume, where the temperature was extremely higher and the lithosphere was thinner (Xia and others, 2003, 2004; Pirajno and others, 2008).

A Mantle Plume Model

Xia and others (2004) suggested that a Carboniferous-Permian mantle plume was once active in NW China including Tarim, Tianshan and Junggar evidenced by the geochemical features of their preferred rift-related volcanic rocks. This model was argued by numerous geological and geochemical observations. Most of the volcanic rocks in their model were formed in marine environment in a large time span when the subduction of the Paleo-Asian Ocean was going on, which has been extensively accepted by most geologists (for example, Qin and others, 2003, 2009; Xiao and others, 2004b, 2009; Zhang and others, 2008; Wang and others, 2009). Furthermore, the Carboniferous period is the main stage for the formation of arc-related porphyry Cu and epithermal Au and basin-related VMS deposits in Tianshan and Circum-Junggar (Qin and others, 2002b, 2005). The mantle plume event discussed in this study is limited spatially within Tianshan, Tarim and Beishan, and temporally in the Early Permian, apparently differing from the plume proposed by Xia and others (2004). Meanwhile, the Early Permian is also the most important ore-forming stage for magmatic Ni-Cu sulfide deposits in Tianshan and Beishan (Qin and others, 2003, 2005, 2009).

Based on the previous studies and the above discussions, we propose a mantle plume model as illustrated in figure 7. In this model, we infer that the Eastern Tianshan and Beishan Rift occur in the inner zone of the plume, since the generation of low-Ti and high-Mg magmas requires extremely high temperature (Nisbet and others, 1993; Herzberg and O'Hara, 2002; Isley and Abbott, 2002; Zhou and others, 2004; Xiao and others, 2004a; Tang and others, 2006) and the rift is attributed to be surface correspondence of the lithospheric uplift overlying the mantle plume (Rogers and others, 2000; Xu and others, 2001; He and others, 2003; Saunders and others, 2005; Zhao and others, 2006). This model can also give good interpretations to the following geological features: (1) Most mafic-ultramafic bodies, particularly in the Eastern Tianshan, extend to the southwest at depth (for example, Xiao and others,

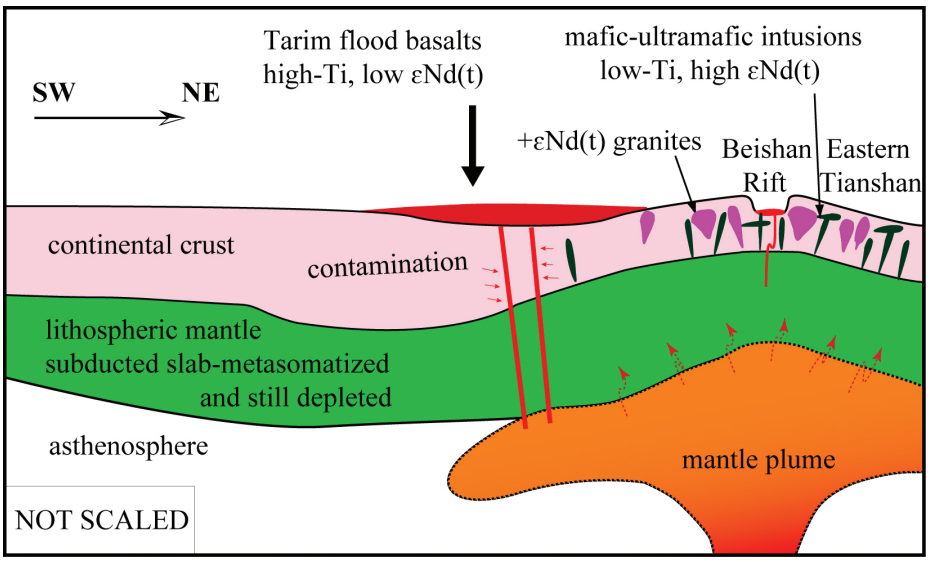

Fig. 7. A possible mantle plume model beneath lithospheric mantle of the Tarim Basin, Tianshan and Beishan. See details in main text.

2010; San and others, 2010), implying that the driving force for the ascending of their parental magmas are the same; (2) The mafic-ultramafic complexes in the Eastern Tianshan and Beishan and basalts in the Tarim Basin have identical formation ages concentrated around 280 Ma (fig. 4; Su and others, 2010b). (3) The geochemical correlations are commonly observed between mafic-ultramafic complexes in Eastern Tianshan and Beishan and basalts in the Tarim Basin (figs. 5 and 6). The Tarim Basin, on the other hand, occurs in the intermediate and outer zones of the plume above which the lithosphere is relatively thicker, and where high-Ti and low-Mg lavas could be produced. Several studies (for example, Zhou and others, 2004; Li and others, 2007; Chai and others, 2008; Mao and others, 2008; Tang and others, 2009; Su and others, 2010b, 2010c; Zhang and others, 2011) have shown that the lithospheric mantle beneath the Tianshan and its adjacent regions had previously been metasomatized by subducted slab but still preserves depletion features, and could be the source of high-Mg magmas forming the mafic-ultramafic intrusions. Similar related geochemical characteristics of the basalts have been described by Chen and others (1997), Zhang and others (2003), Yang and others (2006, 2007a) and Zhou and others (2009). Accordingly, the flood basalts were almost certainly derived from the mantle plume. Underplating of basic magmas beneath the crust could contribute to the generation of the positive $\varepsilon_{Nd}(t)$ and $\varepsilon_{Hf}(t)$ granites (Zhou and others, 2004; Zhang and others, 2008; Su and others, 2010a).

CONCLUSIONS

Zircon U-Pb ages of the mafic-ultramafic intrusions from the Eastern Tianshan and Beishan Rift in this study display restricted range of 278.6 ± 1.2 Ma to 284.0 ± 2.0 Ma. The histogram of compiled published age data of basalts and mafic-ultramafic intrusions generates a peak of 280 Ma which probably represents the time of the mantle plume activity. Geochemically, the basalts have lower $\varepsilon_{Nd}(t)$ ($-9.2\sim-1.7$) and Mg# (<50), and higher TiO_2 contents (mostly >2 wt.%) than the mafic-ultramafic intrusions ($\varepsilon_{Nd}(t) = -1.3\sim11.2$, Mg# = 33~90, $TiO_2 < 1.8$ wt.%), suggesting that the

basalts were generated directly from a peripheral zone of the mantle plume by low degree melting and that the parental magmas of mafic-ultramafic intrusions were produced from lithospheric mantle source by high degree of melting resulting from the higher temperature of the mantle plume head.

Since it is a fundamental model, further studies are required including geochronology to constrain sequence and duration of magma eruption and intrusion, tectonic and sedimentary field surveys for uplift evidence, regional geology survey to constrain the scale of the plume, and geochemistry as well.

ACKNOWLEDGMENTS

This study was financially supported by the Knowledge Innovation Program of the Chinese Academy of Sciences (Grant KZCX2-YW-107), Nature Science Foundation of China (Grant 41030424), and Xinjiang 305 Program (Grant 2006BAB07B03-01). We own debt of gratitude to many geologists who worked in the studying area for their willingness to share freely of their local expertise with us. Discussions with Academician Shu Sun and Zhongli Tang, Professors Jiliang Li, Chusi Li, Wenjiao Xiao, Yigang Xu, Hongfu Zhang, Jun Gao, Yuwang Wang, Changyi Jiang, Zhuangzhi Qian, Xieyan Song, Hong Zhong and Meifu Zhou, and Drs. Guangming Li, Xingwang Xu and Chunming Han were also very helpful. The paper has benefited from constructive reviews by three anonymous reviewers.

References

Ao, S. J., ms, 2010, Paleozoic accretionary tectonics of the Beishan Orogen: insights from anatomy of opiolites and Alaskan-type complexes: Institute of Geology and Geophysics, Chinese Academy of Sciences, Ph. D. thesis (in Chinese with English abstract).

Ao, S. J., Xiao, W. J., Han, C. M., Mao, Q. G., and Zhang, J. E., 2010, Geochronology and geochemistry of Early Permian mafic-ultramafic complexes in the Beishan area, Xinjiang, NW China: Implications for late Paleozoic tectonic evolution of the southern Altaids: Gondwana Research, v. 18, p. 466–478, doi:10.1016/j.gr.2010.01.004.

BGMRXUAR (Bureau of Geology and Mineral Resources of Xinjiang Uygur Autonomous Region), 1993, Regional Geology of Xinjiang Uygur Autonomous Region: Beijing, Geological Press, p. 1–841 (in Chinese).

Campbell, I. H., and Griffiths, R. W., 1990, Implications of mantle plume structure for the evolution of flood basalts: Earth and Planetary Science Letters, v. 99, p. 79–93, doi:10.1016/0012-821X(90)90072-6.

Chai, F. M., Zhang, Z. C., Mao, J. W., Dong, L. H., Zhang, Z. H., and Wu, H., 2008, Geology, petrology and geochemistry of the Baishiquan Ni-Cu-bearing mafic-ultramafic intrusions in Xinjiang, NW China: Implications for tectonics and genesis of ores: Journal of Asian Earth Sciences, v. 32, n. 2–4, p. 218–235, doi:10.1016/j.jseaes.2007.10.014.

Chen, H. L., Yang, S. F., Dong, C. W., Jia, C. Z., Wei, G. Q., and Wang, Z. G., 1997, Confirmation of Permian basite zone in Tarim Basin and its tectonic significance: Geochimica, v. 26, n. 6, p. 77–87 (in Chinese with English abstract).

Chen, H. L., Yang, S. F., Jia, C. Z., Dong, C. W., and Wei, G. Q., 1998, Confirmation of Permian intermediate-acid igneous rock zone and a new understanding of tectonic evolution in the northern part of the Tarim Basin: Acta Mineralogica Sinica, v. 18, p. 370–376 (in Chinese with English abstract).

Chen, H. L., Yang, S. F., and Dong, C. W., 1999, Characteristics and geodynamics of the Early Permian igneous rocks in the Tarim Basin, *in* Chen, H. H., editor, Studies on Collisional Orogenic Belt: Beijing, Ocean Press, p. 174–182 (in Chinese).

Chen, H. L., Yang, S. F., Wang, Q. H., Luo, J. C., Jia, C. Z., Wei, G. Q., Li, Z. L., He, G. Y., and Hu, A. P., 2006, Sedimentary response to the Early-Mid Permian basaltic magmatism in the Tarim plate: Geology in China, v. 33, p. 545–552 (in Chinese with English abstract).

Chen, H. L., Yang, S. F., Li, Z. L., Yu, X., Luo, J. C., He, G. Y., Lin, X. B., and Wang, Q. H., 2009, Spatial and Temporal characteristics of Permian large igneous province in Tarim Basin: Xinjiang Petroleum Geology, v. 30, p. 179–182 (in Chinese with English abstract).

Chen, M. M., Tian, W., Zhang, Z. L., Pan, W. Q., and Song, Y., 2010, Geochronology of the Permian basic-intermediate-acidic magma suit from Tarim, Northwest China and its geological implications: Acta Petrologica Sinica, v. 26, p. 559–572 (in Chinese with English abstract).

Chung, S. L., and Jahn, B. M., 1995, Plume-lithosphere interaction in generation of the Emeishan flood basalts at the Permian-Triassic boundary: Geology, v. 23, p. 889–892, doi:10.1130/0091-7613(1995)023⟨0889:PLIIGO⟩2.3.CO;2.

Coffin, M. F., and Eldholm, O., 1994, Large igneous provinces: crustal structure, dimensions, and external consequences: Reviews of Geophysics, v. 32, n. 1, p. 1–36, doi:10.1029/93RG02508.

Condie, K. C., 2001, Mantle Plumes and Their Record in Earth History: United Kingdom, Oxford, Cambridge University Press, 306 p.

Dalziel, I. W. D., Lawver, L. A., and Murphy, J. B., 2000, Plumes, orogenesis, and supercontinental fragmentation: Earth and Planetary Science Letters, v. 178, p. 1–11, doi:10.1016/S0012-821X(00)00061-3.

Ellam, R. M., and Cox, K. G., 1991, An interpretation of Karoo picrite basalts in terms of interaction between asthenospheric magmas and the mantle lithosphere: Earth and Planetary Science Letters, v. 105, n. 1–3, p. 330–342, doi:10.1016/0012-821X(91)90141-4.

Ellam, R. M., Carlson, R. W., and Shirey, S. B., 1992, Evidence from Re-Os isotopes for plume-lithosphere mixing in Karoo flood basalt genesis: Nature, v. 359, p. 718–721, doi:10.1038/359718a0.

Ernst, R. E., and Buchan, K. L., 2003, Recognizing mantle plumes in the geological record: Annual Review of Earth and Planetary Sciences, v. 31, p. 469–523, doi:10.1146/annurev.earth.31.100901.145500.

Han, B. F., Wang, S. G., Jahn, B. M., Hong, D. W., Kagami, H., and Sun, Y. L., 1997, Depleted-mantle magma source for the Ulungur River A-type granites from north Xinjiang, China: geochemistry and Nd-Sr isotopic evidence, and implications for Phanerozoic crustal growth: Chemical Geology, v. 138, p. 135–159, doi:10.1016/S0009-2541(97)00003-X.

Han, B. F., Ji, J. Q., Song, B., Chen, L. H., and Li, Z. H., 2004, SHRIMP zircon U-Pb ages of Kalatongke No. 1 and Huangshandong Cu-Ni-bearing mafic-ultramafic complexes, North Xinjiang, and geological implications: Chinese Science Bulletin, v. 49, p. 2424–2429, doi:10.1360/04wd0163.

Han, C. M., Xiao, W. J., Zhao, G. C., Ao, S. J., Zhang, J. E., Qu, W. J., and Du, A. D., 2010, In-situ U-Pb, Hf and Re-Os isotopic analyses of the Xiangshan Ni-Cu-Co deposit in Eastern Tianshan (Xinjiang), Central Asia Orogenic Belt: Constraints on the timing and genesis of the mineralization: Lithos, v. 120, p. 547–562, doi:10.1016/j.lithos.2010.09.019.

He, B., Xu, Y. G., Chung, S. L., Xiao, L., and Wang, Y. M., 2003, Sedimentary evidence for a rapid, kilometer-scale crustal doming prior to the eruption of the Emeishan flood basalts: Earth and Planetary Science Letters, v. 213, p. 391–405, doi:10.1016/S0012-821X(03)00323-6.

Herzberg, C., and O'Hara, M. J., 2002, Plume-associated ultramafic magmas of Phanerozoic age: Journal of Petrology, v. 43, n. 10, 1857–1883, doi:10.1093/petrology/43.10.1857.

Isley, A. E., and Abbott, D. H., 2002, Implications of the temporal distribution of high-Mg magmas for mantle plume volcanism through time: The Journal of Geology, v. 110, n. 2, p. 141–158, doi:10.1086/338553.

Jahn, B. M., Wu, F. Y., and Chen, B., 2000a, Massive granitoid generation in Central Asia: Nd isotope evidence and implication for continental growth in the Phanerozoic: Episodes, v. 23, p. 82–92.

——— 2000b, Grantoids of the Central Asian orogenic belt and continental growth in the Phanerozoic: Transactions of the Royal Society of Edinburgh, Earth Sciences, v. 91, n. 1–2, p. 181–193.

Jahn, B. M., Windley, B., Natal'in, B., and Dobretsov, N., 2004, Phanerozoic continental growth in Central Asia: Journal of Asian Earth Sciences, v. 23, n. 5, p. 599–603, doi:10.1016/S1367-9120(03)00124-X.

Jia, C. Z., Wei, G. Q., Yao, H. J., and Li, L. C., 1995, Tectonic Evolution of Tarim and Regional Tectonics: Beijing, Petroleum Industry Press (in Chinese), 174 p.

Jiang, C. Y., Zhang, P. B., Lu, D. R., Bai, K. Y., Wang, Y. P., Tang, S. H., Wang, J. H., and Yang, C., 2004, Petrology, geochemistry and petrogenesis of the Kalpin basalts and their Nd, Sr and Pb isotopic compositions: Geological Review, v. 50, p. 492–500 (in Chinese with English abstract).

Jiang, C. Y., Cheng, S. L., Ye, S. F., Xia, M. Z., Jiang, H. B., and Dai, Y. C., 2006, Lithogeochemistry and petrogenesis of Zhongposhanbei mafic rock body, at Beishan region, Xinjiang: Acta Petrologica Sinica, v. 22, p. 115–126 (in Chinese with English abstract).

Jourdan, F., Bertrand, H., Feraud, G., Le Gall, B., and Watkeys, M. K., 2009, Lithospheric mantle evolution monitored by overlapping large igneous provinces: case study in southern Africa: Lithos, v. 107, n. 3–4, p. 257–268, doi:10.1016/j.lithos.2008.10.011.

Li, H. Q., Chen, F. W., Mei, Y. P., Wu, H., Cheng, S. L., Yang, J. Q., and Dai, Y. C., 2006a, Dating of the No. 1 intrusion of Pobei mafic-ultramafic rocks belt, Xinjiang, and its geological significance: Mineral Deposits, v. 25, n. 4, p. 463–469 (in Chinese with English abstract).

Li, J. X., Qin, K. Z., Xu, X. W., Sun, H., Cheng, S. L., Wu, H., and Mo, X. H., 2007, Geochemistry of Baishiquan Cu-Ni-bearing mafic-ultramafic complex in East Tianshan, Xinjiang: Constraints on ore genesis and tectonic setting: Mineral Deposits, v. 26, n. 1, p. 43–57 (in Chinese with English abstract).

Li, J. Y., Song, B., Wang, K. Z., Li, Y. P., Sun, G. H., and Qi, D. Y., 2006b, Permian mafic-ultramafic complexes on the southern margin of the Tu-Ha Basin, east Tianshan Mountains: geological records of vertical crustal growth in central Asia: Acta Geoscientica Sinica, v. 27, p. 424–446 (in Chinese with English abstract).

Li, Q. L., Li, X. H., Liu, Y., Tang, G. Q., Yang, J. H., and Zhu, W. G., 2010, Precise U-Pb and Pb-Pb dating of Phanerozoic baddeleyite by SIMS with oxygen flooding technique: Journal of Analytical Atomic Spectrometry, v. 25, p. 1107–1113, doi:10.1039/b923444f.

Li, X. H., Liu, Y., Li, Q. L., Guo, C. H., and Chamberlain, K. R., 2009, Precise determination of Phanerozoic zircon Pb/Pb age by multi-collector SIMS without external standardization: Geochemistry Geophysics Geosystems, 10, Q04010, doi:10.1029/2009GC002400.

Li, Y., Su, W., Kong, P., Qian, Y. X., Zhang, K. Y., Zhang, M. L., Chen, Y., Cai, X. Y., and You, D. H., 2007, Zircon U-Pb ages of the Early Permian magmatic rocks in the Tazhong-Bachu region, Tarim Basin by LA-ICP-MS: Acta Petrologica Sinica, v. 23, p. 1097–1107.

Li, Z. L., Yang, S. F., Chen, H. L., Langmuir, C. H., Yu, X., Lin, X. B., and Li, Y. Q., 2008, Chronology and geochemistry of Taxinan basalts from the Tarim Basin: evidence for Permian plume magmatism: Acta Petrologica Sinica, v. 24, p. 959–970 (in Chinese with English abstract).

Liu, P. P., Qin, K. Z., Su, S. G., San, J. Z., Tang, D. M., Su, B. X., Sun, H., and Xiao, Q. H., 2010, Characteristics of multiphase sulfide droplets and their implications for conduit-style mineralization of Tulargen Cu-Ni deposit, eastern Tianshan, Xinjiang: Acta Petrologica Sinica, v. 26, n. 2, p. 523–532 (in Chinese with English abstract).

Ludwig, K. R., 2001, Users manual for Isoplot/Ex rev. 2.49: Berkeley, California, Berkeley Geochronology Centre Special Publication, No. 1a, 56 p.

Mao, J. W., Pirajno, F., Zhang, Z. H., Chai, F. M., Yang, J. M., Wu, H., Chen, S. P., Cheng, S. L., and Zhang, C. Q., 2006b, Late Variscan Post-collisional Cu-Ni sulfide deposits in east Tianshan and Altay in China: principal characteristics and possible relationship with mantle plume: Acta Geologica Sinica, v. 80, p. 925–942.

Mao, J. W., Pirajno, F., Zhang, Z. H., Chai, F. M., Wu, H., Chen, S. P., Cheng, S. L., Yang, J. M., and Zhang, C. Q., 2008, A review of the Cu-Ni sulfide deposits in the Chinese Tianshan and Altay orogens (Xinjiang Autonomous Region, NW China): principal characteristics and ore-forming processes: Journal of Asian Earth Sciences, v. 32, n. 2–4, p. 184–203, doi:10.1016/j.jseaes.2007.10.006.

Mao, Q. G., Xiao, W. J., Han, C. M., Sun, M., Yuan, C., Yan, Z., Li, J. L., Yong, Y., and Zhang, J. E., 2006a, Zircon U-Pb age and geochemistry of the Baishiquan mafic-ultramafic complex in the Eastern Tianshan, Xinjiang province: constraints on the closure of the Paleo-Asian Ocean: Acta Petrologica Sinica, v. 22, p. 153–162 (in Chinese with English abstract).

Nisbet, E. G., Cheadle, M. J., Arndt, N. T., and Bickle, M. J., 1993, Constraining the potential temperature of the Archean mantle: A review of the evidence from komatiites: Lithos, v. 30, n. 3–4, p. 291–307, doi:10.1016/0024-4937(93)90042-B.

Pirajno, F., Mao, J. W., Zhang, Z. C., Zhang, Z. H., and Chai, F. M., 2008, The association of mafic-ultramafic intrusions and A-type magmatism in the Tianshan and Altay orogens, NW China: implications for geodynamic evolution and potential for the discovery of new ore deposits: Journal of Asian Earth Sciences, v. 32, n. 2–4, p. 165–183.

Qin, K. Z., Fang, T. H., Wang, S. L., Zhu, B. Q., Feng, Y. M., Yu, H. F., and Xiu, Q. Y., 2002a, Plate tectonics division, evolution and metallogenic settings in eastern Tianshan mountains, NW China: Xinjiang Geology, v. 20, p. 302–308 (in Chinese with English abstract).

Qin, K. Z., Sun, S., Li, J. L., Fang, T. H., Wang, S. L., and Liu, W., 2002b, Paleozoic epithermal Au and porphyry Cu Deposits in North Xinjiang, China: Epochs, Features, Tectonic Linkage and Exploration Significance: Resource Geology, v. 52, n. 4, p. 291–300, doi:10.1111/j.1751-3928.2002.tb00140.x.

Qin, K. Z., Zhang, L. C., Xiao, W. J., Xu, X. W., Yan, Z., and Mao, J. W., 2003, Overview of major Au, Cu, Ni and Fe deposits and metallogenic evolution of the eastern Tianshan Mountains, Northwestern China, *in* Mao, J. W., Goldfarb, R. J., Seltmann R., Wang, D. W., Xiao, W. J., and Hart, C., editors, Tectonic Evolution and Metallogeny of the Chinese Altay and Tianshan: London, Natural History Museum, International Symposium of the IGCP-473 Project, IAGOD Guidebook Series 10, Urumqi, Xinjiang, China, p. 227–249.

Qin, K. Z., Xiao, W. J., Zhang, L. C., Xu, X. W., Hao, J., Sun, S., and Li, J. L., 2005, Eight stages of major ore deposits in northern Xinjiang, NW-China: Clues and constraints on the tectonic evolution and continental growth of Central Asia, *in* Mao, J. W., and Bierlein, F., editors, Mineral Deposit Research: Meeting the Global Challenge: Springer, v. 1, p. 1327–1330, doi:10.1007/3-540-27946-6-338.

Qin, K. Z., Ding, K. S., Xu, Y. X., Sun, H., Xu, X. W., Tang, D. M., and Mao, Q., 2007, Ore potential of protoliths and modes of Co-Ni occurrence in Tulargen and Baishiquan Cu-Ni-Co deposits, East Tianshan, Xinjiang: Mineral Deposits, v. 26, p. 1–14 (in Chinese with English abstract).

Qin, K. Z, Sun, H., San, J. Z., Xu, X. W., Tang, D. M., Ding, K. S., Xiao, Q. H., and Su, B. X., 2009, Tectonic setting, geological features and evaluation of ore-bearing property for magmatic Cu-Ni deposits in eastern Tianshan, NW China: Proceedings of Xi'an International Ni-Cu(Pt) Deposit Symposium, Northwestern Geology, v. 42, p. 95–99.

Rogers, N., Macdonald, R., Fitton, J. G., George, R., Smith, M., and Barreiro, B., 2000, Two mantle plumes beneath the East African rift system: Sr, Nd and Pb isotope evidence from Kenya Rift basalts: Earth and Planetary Science Letters, v. 176, p. 387–400, doi:10.1016/S0012-821X(00)00012-1.

San, J. Z., Qin, K. Z., Tang, Z. L., Tang, D. M., Su, B. X., Sun H., Xiao, Q. H., and Liu, P. P., 2010, Precise zircon U-Pb age dating of two mafic-ultramafic complexes at Tulargen large Cu-Ni district and its geological implications: Acta Petrologica Sinica, v. 26, p. 3027–3035 (in Chinese with English abstract).

Saunders, A. D., Storey, M., Kent, R. W., and Norry, M. J., 1992, Consequences of plume-lithosphere interactions: Geological Society, London, Special Publications, v. 68, p. 41–60, doi:10.1144/GSL.SP.1992.068.01.04.

Saunders, A. D., England, R. W., Reichow, M. K., and White, R. V., 2005, A mantle plume origin for the Siberian traps: uplift and extension in the West Siberian Basin, Russia: Lithos, v. 79, p. 407–424, doi:10.1016/j.lithos.2004.09.010.

Stacey, J. S., and Kramers, J. D., 1975, Approximation of terrestrial lead isotope evolution by a two-stage model: Earth and Planetary Science Letters, v. 26, p. 207–221, doi:10.1016/0012-821X(75)90088-6.

Storey, B. C., Leat, P. T., Weaver, S. D., Pankhurst, R. J., Bradshaw, J. D., and Kelley, S., 1999, Mantle plumes and Antarctica–New Zealand rifting: evidence from mid-Cretaceous mafic dykes: Journal of the Geological Society, London, v. 156, p. 659–672, doi:10.1144/gsjgs.156.4.0659.

Su, B. X., Qin, K. Z., Sun, H., Tang, D. M., Xiao, Q. H., and Cao, M. J., 2009, Petrological and mineralogical characteristics of Hongshishan mafic-ultramafic complex in Beishan area, Xinjiang: implications for assimilation and fractional crystallization: Acta Petrologica Sinica, v. 25, p. 873–887 (in Chinese with English abstract).

Su, B. X., Qin, K. Z., Sakyi, P. A., Liu, P. P., Tang, D. M., Malaviarachchi, S. P. K., Xiao, Q. H., Sun, H., Dai, Y. C., and Hu, Y., 2010a, Geochemistry and geochronology of acidic rocks in the Beishan region, NW China: petrogenesis and tectonic implications: Journal of Asian Earth Sciences, v. 41, p. 31–43, doi:10.1016/j.jseaes.2010.12.002.

Su, B. X., Qin, K. Z., Sakyi, P. A., Li, X. H., Yang, Y. H., Sun, H., Tang, D. M., Liu, P. P., Xiao, Q. H., and Malaviarachchi, S. P. K., 2010b, U-Pb ages and Hf-O isotopes of zircons from Late Paleozoic mafic-ultramafic units in the southern Central Asian Orogenic Belt: Tectonic implications and evidence for an Early-Permian mantle plume: Gondwana Research, doi:10.1016/j.gr.2010.11.015.

Su, B. X., Qin, K. Z., Sakyi, P. A., Tang, D. M., Liu, P. P., Malaviarachchi, S. P. K., Xiao, Q. H., and Sun, H., 2010c, Geochronologic-petrochemical studies of the Hongshishan mafic-ultramafic intrusion, Beishan area, Xinjiang (NW China): petrogenesis and tectonic implications: International Geology Review, doi:10.1080/00206814.2010.543011.

Su, B. X., Qin, K. Z., Sun, H., and Wang, H., 2010d, Geochronological, petrological, mineralogical and geochemical studies of the Xuanwoling mafic-ultramafic intrusion in the Beishan area, Xinjiang: Acta Petrologica Sinica, v. 26, p. 3283–3294 (in Chinese with English abstract).

Su, B. X., Qin, K. Z., Sakyi, P. A., Malaviarachchi, S. P. K., Liu, P. P., Tang, D. M., Xiao, Q. H., Sun, H., Ma, Y. G., and Mao, Q., 2010e, Occurrence of an Alaskan-type complex in the Middle Tianshan Massif, Central Asian Orogenic Belt: inferences from petrological and mineralogical studies: International Geology Review, doi:10.1080/00206814.20 10.543009.

Sun, H., ms, 2009, Ore-forming mechanism in conduit system and ore-bearing property evaluation for mafic-ultramafic complex in Eastern Tianshan, Xinjiang: Beijing, China, Institute of Geology and Geophysics, Chinese Academy of Sciences, Ph. D. dissertation (in Chinese with English abstract).

Sun, H., Qin, K. Z., Li, J. X., Xu, X. W., San, J. Z., Ding, K. S., Hui, W. D., and Xu, Y. X., 2006, Petrographic and geochemical characteristics of the Tulargen Cu-Ni-Co sulfide deposits, East Tianshan, Xinjiang, and its tectonic setting: Geology in China, v. 33, p. 606–617 (in Chinese with English abstract).

Sun, H., Qin, K. Z., Xu, X. W., Li, J. X., Ding, K. S., Xu, Y. X., and San, J. Z., 2007, Petrological characteristics and copper-nickel ore-forming processes of early Permian mafic-ultramafic intrusion belts in east Tianshan: Mineral Deposits, v. 26, p. 98–108 (in Chinese with English abstract).

Tang, D. M., Qin, K. Z., Sun, H., Su, B. X., Xiao, Q. H., Cheng, S. L., and Li, J., 2009, Zircon U-Pb age and geochemical characteristics of Tianyu intrusion, East Tianshan: Constraints on source and genesis of mafic-ultramafic intrusions in East Xinjiang: Acta Petrologica Sinica, v. 25, p. 817–831 (in Chinese with English abstract).

Tang, Y. J., Zhang, H. F., and Ying, J. F., 2006, Asthenosphere-lithospheric mantle interaction in an extensional regime: implication from the geochemistry of Cenozoic basalts from Taihang Mountains, North China Craton: Chemical Geology, v. 233, p. 309–327, doi:10.1016/j.chemgeo.2006.03.013.

Tian, W., Campbell, I. H., Allen, C. M., Guan, P., Pan, W. Q., Chen, M. M., Yu, H. J., and Zhu, W. P., 2010, The Tarim picrite-basalt-rhyolite suite, a Permian flood basalt from northwest China with contrasting rhyolites produced by fractional crystallization and anatexis: Contributions to Mineralogy and Petrology, v. 160, n. 3, p. 407–425, doi:10.1007/s00410-009-0485-3.

Wang, T., Jahn, B. M., Kovach, V. P., Tong, Y., Hong, D. W., and Han, B. F., 2009, Nd-Sr isotopic mapping of the Chinese Altai and implications for continental growth in the Central Asian Orogenic Belt: Lithos, v. 110, n. 1–4, p. 359–372, doi:10.1016/j.lithos.2009.02.001.

Wang, Y. W., Wang, J. B., Wang, L. J., and Long, L. L., 2009, Characteristics of two mafic-ultramafic rock series in the Xiangshan Cu-Ni-(V) Ti-Fe ore district, Xinjiang: Acta Petrologica Sinica, v. 25, n. 4, p. 888–900 (in Chinese with English abstract).

Weaver, S. D., Storey, B. C., Pankhurst, R. J., Mukasa, S. B., DiVenere, V. J., and Bradshaw, J. D., 1994, Antarctica–New Zealand rifting and Marie Byrd Land lithospheric magmatism linked to ridge subduction and mantle plume activity: Geology, v. 22, n. 9, p. 811–814, doi:10.1130/0091-7613(1994)022⟨0811:ANZRAM⟩2.3.CO;2.

Wu, H., Li, H. Q., Mo, X. H., Chen, F. W., Lu, Y. Y., Mei, Y. P., and Deng, G., 2005, Age of the Baishiquan mafic-ultramafic complex, Hami, Xinjiang and its geological significance: Acta Geologica Sinica, v. 79, p. 498–502 (in Chinese with English abstract).

Xia, L. Q., Xu, X. Y., Xia, Z. C., Li, X. M., Ma, Z. P., and Wang, L. S., 2003, Carboniferous post-collisional rift volcanism of the Tianshan Mountains, northwestern China: Acta Geologica Sinica, v. 77, n. 3, p. 338–360, doi:10.1111/j.1755-6724.2003.tb00751.x.

——— 2004, Petrogenesis of Carboniferous rift-related volcanic rocks in the Tianshan, northwestern China: Geological Society of America Bulletin, v. 116, n. 3–4, p. 419–433, doi:10.1130/B25243.1.

Xia, L. Q., Li, X. M., Xia, Z. C., Xu, X. Y., Ma, Z. P., and Wang, L. S., 2006, Carboniferous-Permian rift-related volcanism and mantle plume in the Tianshan, northwestern China: Northwestern Geology, v. 39, p. 1–49 (in Chinese with English abstract).

Xia, M. Z., Jiang, C. Y., Qian, Z. Z., Sun, T., Xia, Z. D., and Lu, R. H., 2008, Geochemistry and petrogenesis for Hulu intrusion in East Tianshan, Xinjiang: Acta Petrologica Sinica, v. 24, p. 2749–2760 (in Chinese with English abstract).

Xiao, L., Xu, Y. G., Chung, S. L., He, B., and Mei, H. J., 2003, Chemostratigraphic correlation of upper Permian lavas, from Yunnan Province, China: extent of the Emeishan large igneous province: International Geology Review, v. 45, n. 8, p. 754–766, doi:10.2747/0020-6814.45.8.753.

Xiao, L., Xu, Y. G., Mei, H. J., Zheng, Y. F., He, B., and Pirajno, F., 2004a, Distinct mantle sources of low-Ti and high-Ti basalts from the western Emeishan large igneous province, SW China: implications for plume-lithosphere interaction: Earth and Planetary Science Letters, v. 228, n. 3–4, p. 525–546, doi: 10.1016/j.epsl.2004.10.002.

Xiao, Q. H., Qin, K. Z., Su, B. X., Sun, H., Tang, D. M., and Cao, M. J., 2010, Studies on Xiangshan Ti-Fe and Ni-Cu sulfide ore bearing mafic-ultramafic complex from eastern Tianshan, Xinjiang: Acta Petrologica Sinica, v. 26, p. 503–522 (in Chinese with English abstract).

Xiao, W. J., Zhang, L. C., Qin, K. Z., Sun, S., and Li, J. L., 2004b, Paleozoic accretionary and collisional tectonics of the eastern Tianshan (China): Implications for the continental growth of central Asia: American Journal of Science, v. 304, p. 370–395, doi:10.2475/ajs.304.4.370.

Xiao, W. J., Windley, B. F., Yuan, C., Sun, M., Han, C. M., Lin, S. F., Chen, H. L., Yan, Q. R., Liu, D. Y., Qin, K. Z., Li, J. L., and Sun, S., 2009, Paleozoic multiple subduction-accretion processes of the southern Altaids: American Journal of Science, v. 309, p. 221–270, doi:10.2475/03.2009.02.

Xu, X. Y., He, S. P., Wang, H. L., and Chen, J. L., 2009, Geological Background Map of Mineralization in Eastern Tianshan-Beishan Area (in Chinese).

Xu, Y. G., Chung, S. L., Jahn, B. M., and Wu, G. Y., 2001, Petrologic and geochemical constraints on the petrogenesis of Permian-Triassic Emeishan flood basalts in southwestern China: Lithos, v. 58, p. 145–168, doi:10.1016/S0024-4937(01)00055-X.

Yang, S. F., Chen, H. L., Dong, C. W., Jia, C. Z., and Wang, Z. G., 1996, The discovery of Permian syenite inside Tarim basin and its geodynamic significance: Geochimica, v. 25, p. 121–128 (in Chinese with English abstract).

Yang, S. F., Chen, H. L., Ji, D. W., Li, Z. L., Dong, C. W., Jia, C. Z., and Wei, G. Q., 2005, Geological process of Early to Middle Permian magmatism in Tarim Basin and its geodynamic significance: Geological Journal of China Universities, v. 11, p. 504–511 (in Chinese with English abstract).

Yang, S. F., Li, Z. L., Chen, H. L., Santosh, M., Dong, C. W., and Yu, X., 2007a, Permian bimodal dyke of Tarim Basin, NW China: Geochemical characteristics and tectonic implications: Gondwana Research, v. 12, p. 113–120, doi:10.1016/j.gr.2006.10.018.

Yang, S. F., Yu, X., Chen, H. L., Li, Z. L., Wang, Q. H., and Luo, J. C., 2007b, Geochemical characteristics and petrogenesis of Permian Xiaohaizi ultrabasic dyke in Bachu area, Tarim Basin: Acta Petrologica Sinica, v. 23, p. 1087–1096 (in Chinese with English abstract).

Yang, S. F., Li, Z. L., Chen, H. L., Chen, W., and Yu, X., 2006, ^{40}Ar-^{39}Ar dating of basalts from Tarim Basin, NW China and its implication to a Permian thermal tectonic event: Journal of Zhejiang University—Science, A7, p. 320–324, doi:10.1631/jzus.2006.AS0320.

Zhang, C. L., Li, X. H., Li, Z. X., Ye, H. M., and Li, C. N., 2008, A Permian layered intrusive complex in the Western Tarim Block, northwestern China: product of a ca. 275-Ma mantle plume?: The Journal of Geology, v. 116, n. 3, p. 269–287, doi:10.1086/587726.

Zhang, M. J., Li, C. S., Fu, P. E., Hu, P. Q., and Ripley, E. M., 2011,The Permian Huangshanxi Cu-Ni deposit in western China: Intrusive-extrusive association, ore genesis and exploration implications: Mineralium Deposita, v. 46, n. 2, p. 153–170, doi:10.1007/s00126-010-0318-3.

Zhang, S. B., Ni, Y. N., and Gong, F. H., 2003, A Guide to the Stratigraphic Investigation on the Periphery of the Tarim Basin: Beijing, Petroleum Industry Press, 280 p.

Zhang, Y. T., Liu, J. Q., and Guo, Z. F., 2010, Permian basaltic rocks in the Tarim basin, NW China: implications for plume-lithosphere interaction: Gondwana Research, v. 18, n. 4, p. 596–610, doi:10.1016/j.gr.2010.03.006.

Zhao, D. P., Lei, J. S., Inoue, T., Yamada, A., and Gao, S. S., 2006, Deep structure and origin of the Baikal rift zone: Earth and Planetary Science Letters, v. 243, n. 3–4, p. 681–691, doi:10.1016/j.epsl.2006.01.033.

Zhong, H., and Zhu, W. G., 2006, Geochronology of layered mafic intrusions from the Pan-Xi area in the Emeishan large igneous province, SW China: Mineralium Deposita, v. 41, n. 6, p. 599–606, doi:10.1007/s00126-006-0081-7.

Zhong, H., Yao, Y., Hu, S. F., Zhou, X. H., Liu, B. G., Sun, M., Zhou, M.-F., and Viljoen, M. J., 2003, Trace-element and Sr-Nd isotopic geochemistry of the PGE-bearing Hongge layered intrusion, Southwestern China: International Geology Review, v. 45, p. 371–382, doi:10.2747/0020-6814.45.4.371.

Zhong, Y. T., and Xu, Y. G., 2009, Characteristics of plume-related A-type granites: an example from the Emeishan large igneous province: Journal of Jilin University (Earth Science Edition), v. 39, p. 828–838 (in Chinese with English abstract).

Zhou, M. F., Lesher, C. M., Yang, Z. X., Li, J. W., and Sun, M., 2004, Geochemistry and petrogenesis of 270 Ma Ni-Cu-(PGE) sulfide-bearing mafic intrusions in the Huangshan district, Eastern Xinjiang, Northwest China: implications for the tectonic evolution of the Central Asian orogenic belt: Chemical Geology, v. 209, n. 3–4, p. 233–257, doi:10.1016/j.chemgeo.2004.05.005.

Zhou, M. F., Arndt, N. T., Malpas, J., Wang, C. Y., and Kennedy, A. K., 2008, Two magma series and associated ore deposit types in the Permian Emeishan large igneous province, SW China: Lithos, v. 103, n. 3–4, p. 352–368, doi:10.1016/j.lithos.2007.10.006.

Zhou, M. F., Zhao, J. H., Jiang, C. Y., Gao, J. F., Wang, W., and Yang, S. H., 2009, OIB-like, heterogeneous mantle sources of Permian basaltic magmatism in the western Tarim Basin, NW China: implications for a possible Permian large igneous province: Lithos, v. 113, p. 583–594, doi:10.1016/j.lithos.2009.06.027.

Zindler, A., and Hart, S. R., 1986, Chemical geodynamics: Annual Review of Earth and Planetary Sciences, v. 14, p. 493–571, doi:10.1146/annurev.ea.14.050186.002425.